ND70 series basaltic glass reference materials for volatile element (H_2O, CO_2, S, Cl, F) analysis and the C ionisation efficiency suppression effect of water in silicate glasses in SIMS analysis.

Yves Moussallam[1], William Henry Towbin[2], Terry Plank[1], Hélène Bureau[3], Hicham Khodja[4], Yunbin Guan[5], Chi Ma[5], Michael B. Baker[5], Edward M. Stolper[5], Fabian U. Naab[6], Brian D. Monteleone[7], Glenn G. Gaetani[7], Hyun Joo Lee[1], Shuo Ding[1], Sarah Shi[1], Estelle F. Rose-Koga[8].

[1] Lamont-Doherty Earth Observatory, Columbia University, New York, USA

[2] Gemological Institute of America, 50 W. 47th Street, New York, NY 10036, United States of America

[3] IMPMC, Sorbonne Université, CNRS UMR 7590, MNHN, IRD UR 206, 4 place Jussieu, 75252 Paris Cedex 05, France

[4] LEEL, NIMBE, CEA, CNRS, Université Paris−Saclay, CEA Saclay, 91191 Gif sur Yvette Cedex, France

[5] Division of Geological and Planetary Sciences, California Institute of Technology, Pasadena, California 91125, USA

[6] Department of Nuclear Engineering and Radiological Sciences, University of Michigan, Ann Arbor, Michigan 48109, USA

[7] Department of Geology and Geophysics, Woods Hole Oceanographic Institution, Woods Hole, MA 02543, USA.

[8] ISTO, UMR 7327, CNRS-UO-BRGM, 1A rue de la Férollerie, 45071 Orléans cedex 2, France

Corresponding author: Yves Moussallam; yves.moussallam@ldeo.columbia.edu

The paper is a non-peer reviewed preprint submitted to EarthArXiv. This manuscript has been submitted to Geostandards and Geoanalytical research and is currently under peer review there.

ABSTRACT

We present a new set of reference material, the ND70-series, for in situ analysis of volatile elements (H_2O, CO_2, S, Cl, F) in silicate glass of basaltic composition. Samples have been synthesised in piston cylinders at pressures of 1 to 1.5 GPa at volatile-undersaturated conditions. They span concentrations from 0 to 6 wt.% H_2O, from 0 to 1.6 wt.% CO_2 and from 0 to 1 wt.% S, Cl and F. The samples have been characterised by Elastic Recoil Detection Analysis (ERDA) for H_2O, by Nuclear Reaction Analysis (NRA) for CO_2, by Elemental Analyser (EA) for CO_2, by Fourier Transform Infrared Spectroscopy (FTIR) for H_2O and CO_2, by Secondary Ion Mass Spectrometry (SIMS) for H_2O, CO_2, S, Cl and F, and by Electron Microprobe (EMP) for CO_2, S, Cl, and major elements. Comparison between expected and measured volatile amounts across techniques and institutions is excellent. It was found however that SIMS analyses of CO_2 concentrations using either Cs^+ or O^- primary beams are strongly affected by the glass H_2O content. Reference materials are being distributed at Ion probe facilities in the US, Europe and Japan. Remaining reference materials will be deposited at the Smithsonian National Museum of Natural History where they will be freely available on loan to any researcher.

I. INTRODUCTION

Volatile elements (C-O-H-S-Cl-F) play a major role in planetary processes including habitability (e.g., Ehlmann et al., 2016; Foley & Smye, 2018; Dehant et al., 2019), plate tectonics (e.g., Albarède, 2009; Stern, 2018; Nicoli & Ferrero, 2021), mantle melting (e.g., Wyllie, 1971; Eggler, 1976; Dasgupta & Hirschmann, 2006) and volcanic eruptions (e.g., Elskens et al., 1968; Allard, 2010; Edmonds & Woods, 2018). Understanding the planetary-scale cycling of volatiles has hence long been a subject of interest to geoscientists. Critical to that effort is the ability to reliably measure volatiles in geological materials. For volcanologists, igneous petrologists and mantle geochemists, the ability to measure volatile elements in melts (i.e., glasses) and mineral-hosted melt inclusions is of particular interest (e.g., Dixon et al., 1988; Hauri et al., 2002; Métrich & Wallace, 2008). Secondary Ion Mass Spectrometry (SIMS) is a technique that allows for the simultaneous measurements of all major volatile species in silicate glasses (e.g., Shimizu et al., 2017). One persistent issue with SIMS analyses however is that the ionization efficiency varies by element, primary beam, and major element matrix. To be fully quantitative, the technique hence requires well characterized reference materials with bulk compositions similar to that of the sample. To date, ion microprobe facilities in Nancy, Paris, Lausanne, Edinburgh, Washington, Woods Hole, Pasadena, Tempe and Kochi, amongst other, have all either acquired or synthesised their own sets of reference material for volatile elements in basaltic glasses. Although sharing natural standards is quite common (e.g., Shimizu et al., 2017), efforts to synthesize a large amounts of glasses and to cross-calibrate instruments prior to using the synthetic glasses as standards have been quite limited, particularly on an international scale. This has resulted in significant challenges when attempting to directly compare analytical results generated by different facilities. Furthermore, not all of these facilities possess reference materials that span the entire range of volatile concentrations found in geological samples. As a consequence, some measurements are reliant on extrapolation from calibration curves. In this context, we introduce and thoroughly characterize a new series of synthetic basaltic glasses. These glasses are intended to serve as international reference materials for the analysis of H_2O, CO_2, S, Cl, and F concentrations in natural glasses with a basaltic composition, particularly in the context of SIMS and other micro-beam techniques.

II. EXPERIMENTAL METHOD

We used as starting material a natural Back-Arc-Basin-Basalt, ND-70, dredged at Lat:15º 52' S, Lon:174º51' W from a depth of 2500 m b.s.l. (Keller et al., 2008) at the Mangatolu Triple Junction

in the northern Lau back-arc region (initial composition: 49.2 wt.% SiO_2, 0.8 wt.% TiO_2, 16.1wt.% Al_2O_3, 7.9 wt.% FeO_{tot}, 8.2 wt.% MgO, 12.8 wt.% CaO, 1.9 wt.% Na_2O, 0.15 wt.% K_2O, 0.1 wt.% P_2O_5, 889 ppm S, 219 ppm Cl, 1.02 wt.% H_2O, 76 ppm CO_2, and 148 ppm F; Keller et al., 2008; Caulfield et al., 2012; Lloyd et al., 2013). Five grams of material were crushed, placed in a platinum crucible and fused at 0.1MPa, in air, at 1350 °C for two hours, quenched in water (without submersing the crucible), crushed and mixed again and fused a second time at 1350 °C, 0.1MPa, in air, for an additional two hours and quenched again in water (without submersing the crucible). This volatile-free glass (ND70-degassed) constitutes the first sample in our standard suite (i.e., the blank), and was then used as the starting powder for subsequent piston cylinder experiments.

High-pressure experiments were prepared by adding powdered ND70-degassed glass with the desired amounts of H_2O, CO_2, S, Cl and F in $Au_{80}Pd_{20}$ capsules which were then welded shut. H_2O was loaded as liquid deionized water (using a micro-pipette), CO_2 was loaded as powdered calcite ($CaCO_3$), S was loaded as anhydrite ($CaSO_4$), Cl was loaded as halite (NaCl) and F was loaded as Sellaite (MgF_2). Table 1 gives the intended composition of each experiment based on the added weight of each component (given in Table S1). High-pressure experiments were all performed in a piston cylinder apparatus at the Lamont-Doherty Earth Observatory (LDEO). We used a 1/2-inch assembly composed of a CaF_2 pressure cell, a graphite furnace, and MgO sleeves and spacer surrounding the ($Ø_{ext}$ = 5.0 mm, $Ø_{int}$ = 4.8 mm, length = 8.0 mm) $Au_{80}Pd_{20}$ capsule. The temperature was monitored with a D-type ($W_{97}Re_3$-$W_{75}Re_{25}$) thermocouple, separated from the capsule by a 0.8 mm alumina disc. No attempt at controlling oxygen fugacity was made, although given that our starting powder (ND70-degassed) was fused in air, we assume highly oxidised conditions. Run conditions for each experiment are reported in Table 2. Piston cylinder experiments were conducted at pressures of 1 and 1.5 GPa, temperatures of 1225 and 1325°C and equilibrated for 2 h. Experiments were quenched by turning off the electric power and took approximately 5 s to cool bellow 400 °C. An additional experiment, INSOL_MX1_BA4, was run using a powdered mixture of natural basalt (60%) and dacite (30%) (from Kilauea and Tutupaca volcanoes, respectively, Moussallam et al., unpublished) with dolomite (10%) following the same piston cylinder methodology as described above and equilibrated at 1GPa and 1275˚C for 2h. No additional water, S, Cl nor F was added. Initial CO_2 loaded was far above saturation. Finally another experiment VILLA_P2 was run using a powdered mixture of natural basaltic andesite from Villarrica volcano (same starting material as described in Moussallam et al., 2023) to which deionized water, elemental sulfur and oxalic acid dihydrate were added such that the initial concentrations of CO_2 and S would be above saturation level (based on previous experiments on similar composition) at the conditions of the experiment. The charge was run in an internally heated

pressure vessel at the American Museum of Natural History and equilibrated at 300 MPa, 1150˚C for 2h at the intrinsic fO_2 of the vessel (~NNO+2; Webster et al., 2011). Both INSOL_MX1_BA4 and VILLA_P2 are not part of the reference material suite that we present here as they were not synthesised in sufficient quantities but were used for calibration purposes during some of the SIMS sessions discussed below. All samples were entirely glassy excepted ND70-4-01 which partially crystalised on one side of the capsule (partially crystallized portion was mechanically removed).

III. ANALYTICAL TECHNIQUES

Experiments were analysed by Elastic Recoil Detection Analysis (ERDA) for H_2O, by Nuclear Reaction Analysis (NRA) for CO_2, by Elemental Analyser (EA) for CO_2, by Fourier Transform Infrared Spectroscopy (FTIR) for H_2O and CO_2, by Secondary Ion Mass Spectrometry (SIMS) for H_2O, CO_2, S, Cl and F, and by Electron Microprobe (EMP) for CO_2, S, Cl and major elements.

a) Nuclear Microprobe (ERDA and NRA)

H_2O and CO_2 absolute concentrations were evaluated using two Ion Beam Analysis techniques, namely Elastic Recoil Detection Analysis (ERDA) and Nuclear Reaction Analysis (NRA). Measurements were performed at the Laboratoire d'Etude des Eléments Légers (LEEL) joint CEA-CNRS laboratory in Saclay (Khodja et al., 2001) where these techniques are regularly employed to quantify light elements in various materials, including geological samples (Clesi et al., 2018; Malavergne et al., 2019). H_2O was analysed as H by ERDA following the approaches described in Bureau et al., (2009). We used a $^4He^+$ ion beam at 2.7 MeV energy that interacts with the samples at grazing incidence. A 12 μm Mylar absorber was mounted between the sample and the forward (30°) particle detector to stop all scattered $^4He^+$ and let recoil H^+ ions reach the detector. CO_2 was analysed as C by NRA, making use of the sensitive $^{12}C(d,p)^{13}C$ nuclear reaction at 170° detection angle using a deuteron ($^2H^+$) microbeam at 1.4 MeV. Although no absorber was used, detected protons, in the 2750–3150 keV energy range, are far above backscattered deuterons. Quantification was performed by precisely measuring detector solid angles using reference materials and by adjusting experimental spectra with the SIMNRA software (Mayer, 1999). The parasitic contribution from the $^{28}Si(d,p)^{29}Si$ was systematically subtracted using a Suprasil reference spectrum (H_2O<1 ppm; e.g., Shimizu et al., 2019).

b) Elemental Analyser

We used a Costech elemental analyzer (ECS4010) at the Lamont−Doherty Earth Observatory to measure CO_2 (as C) in the two most CO_2-rich experiments (with > 1 wt% CO_2). Hand-picked glass samples were precisely weighed on a microbalance with a precision of ± 0.001 mg, and then wrapped in 3.2 × 4 mm tin foil envelopes. These encapsulated samples were subjected to combustion (at ~1700 °C) over a chromium (III) oxide catalyst with excess oxygen (25 mL/min). The carrier gas was helium, flowing at a rate of 100 mL/min. To ensure complete oxidation of sample carbon into CO_2 and the elimination of remaining halogens or sulfur, silvered cobaltous/cobaltic oxide, positioned lower in the quartz combustion tube, was used. The analyser was calibrated directly prior to sample analysis using mixtures of oxalic acid and SiO_2 with 1, 2, 5, 20, and 70 wt% of CO_2. This calibration (R^2 = 0.9999; Fig. S1) was then used to determine the CO_2 content of the samples. Error on C was estimated at ±2% (±7.3% on CO_2) based on reproducibility of external standards (calcite and dolomite) similar to other studies using elemental analyser in silicate glasses (e.g., Moussallam et al., 2015, 2016).

c) Fourier Transform Infrared Spectroscopy (FTIR)

H_2O and CO_2 concentrations in doubly polished experimental glasses were measured using a N_2 purged Thermo Scientific Nicolet iN10 mx Fourier Transform Infrared Spectrometer (FTIR) at LDEO. Measurements were collected with aperture sizes varying between 100 × 100 µm and 200 × 200 µm. Thickness of the doubly polished wafers were measured using a digital micrometer (Mitutoyo Digimatic Indicator) and calculated using the "interference fringe" method (Tamic et al., 2001) that requires determining the wavelength of interference fringes of reflectance spectra collected from the sample. The latter method enables determining the thickness at the same spot where the transmission spectra is collected. Several spots were measured on each glass to ensure no heterogeneity. Baseline fitting, density calculations, absorption coefficients and ultimately H_2O and CO_2 concentration were determined using PyIRoGlass (Shi et al., in review; https://github.com/sarahshi/PyIRoGlass), except for INSOL_MX1_BA4 where we used the spectra obtained from a de-volatised (i.e., fused twice at 0.1MPa in air for 2h) version of the same composition to define the baseline.

d) Secondary Ion Mass Spectrometry at CNRS-Nancy

A first indium mount with all experimental glasses pressed was cleaned with DI and Millipore filtered water, dried and then coated with a ~20 nm Au layer. Volatile (H_2O, CO_2, Cl, F, S) contents in experimental glasses were determined using a Cameca IMS 1280 ion microprobe

at CRPG-CNRS-Nancy, France. We used a Cs^+ primary beam with a current of 1 nA and an electron gun to compensate for charge build-up at the sample surface. A 180 s pre-sputter with a 30 × 30 µm square raster was applied, then analyses were performed on the 15 to 20 µm spot in the center of the rastered clean area using a mechanical aperture placed at the secondary ion image plane. Analyses were performed in multi-collector mode; CO_2, H_2O, F, Cl and S were measured using an electron multiplier, while Si and O were measured on a faraday cup. We collected signals for ^{12}C (8 s), ^{17}O (3 s), $^{16}O^1H$ (6 s), ^{18}O (3 s), ^{19}F (4 s), ^{27}Al (3 s), ^{30}Si (3 s), ^{32}S (4 s) and ^{35}Cl (6 s; counting times in parentheses), with 2 s waiting time after each switch of the magnet. This cycle was repeated 10 times during one analysis for a total analysis duration of 12 minutes. The mass resolution of ~7000 (with the contrast aperture at 400 µm, the energy aperture at 40 eV, the entrance slit at 52 µm and the exit slit at 173 µm) meant that complete discrimination of the following mass interferences was achieved: $^{34}S^1H$ on ^{35}Cl; ^{17}O on $^{16}O^1H$; $^{29}Si^1H$ on ^{30}Si; $^{31}P^1H$ on ^{32}S.

Together with our experimental glasses, we measured natural and experimental basaltic glasses KL2G (Jochum et al. 2006) KE12 (Mosbah et al. 1991), VG2 (Jarosewich et al. 1980), experimental glasses N72, M34, M35, M40, M43 and M48 (Shishkina et al. 2010), and the Macquarie glasses 40428 and 47963 (Kamenetsky et al. 2000) under the same analytical conditions at the beginning and end of the session. The Calibration lines are shown in Fig. S2. All existing standard values are reported in Table S2.

e) Secondary Ion Mass Spectrometry at Woods Hole Oceanographic Institution

A second indium mount containing different set of chips of experimental glasses pressed, was cleaned with DI and Millipore filtered water, dried and then coated with a ~20 nm Au layer. Volatile concentration analyses were conducted on a Cameca ims1280 at the Northeast National Ion Microprobe Faciltiy (NENIMF) at the Woods Hole Oceanographic Institution. The standards were measured in separate sessions using a $^{133}Cs^+$ primary beam, then a $^{16}O^-$ primary beam.

Cs SIMS measurements:

A 500pA – 1nA $^{133}Cs^+$ primary ion beam, accelerated 10kV, was focused to a 10-15 µm diameter, then rastered to produce a ~25 x 25 µm crater. Secondary ions ($^{12}C^-$, $^{16}OH^-$, $^{18}O^-$, $^{19}F^-$, $^{30}Si^-$, $^{31}P^-$, $^{32}S^-$ and $^{35}Cl^-$) were extracted with a 10kV voltage potential. The extracted and magnified secondary ions were centered through a 600 x 600 µm mechanical field aperture, which blocked transmission of secondary ions from outside of the central ~7.5 x 7.5 µm the

measurement crater. The secondary field aperture is necessary to minimize the transmission of background and surficial volatile ions residing the sample chamber, the surrounding sample surface, and within the outer edges of the sputtering crater. A normal-incidence electron gun set at -10kV was used to compensate for positive electron charge buildup around the sample crater. The energy bandwidth for the secondary ions was ~60 eV. A mass resolving power > 5500 was used to separate interfering masses, such as $^{17}O^-$ from $^{16}OH^-$. Each measurement consisted of 180 seconds of presputtering, automatic secondary beam centering, and automatic mass calibration, followed by five cycles of counting of each ion intensity on an ETP electron multiplier in magnet peak jumping mode. Count times in seconds for each mass were as follows: $^{12}C^- = 10$, $^{16}OH^- = 5$, $^{18}O^- = 3$, $^{19}F^- = 5$, $^{30}Si^- = 3$, $^{31}P^- = 5$, $^{32}S^- = 5$, $^{35}Cl^- = 5$. Background intensities were measured on Suprasil 3002 glass for C, OH, F, P, and S, and on Herasil glass for Cl.

O^- SIMS measurements:

A 10nA $^{16}O^-$ primary ion beam, accelerated 13kV, was focused to a ~25 µm diameter, then rastered to produce a ~30 – 35 µm diameter crater. Secondary ions ($^{12}C^+$, $^{16}O^+$, $^{16}OH^+$, $^{19}F^+$, $^{30}Si^+$, $^{31}P^+$, $^{32}S^+$ and $^{35}Cl^+$) were extracted with a 10kV voltage potential. A 1250 x 1250 µm mechanical field aperture was set to blocked transmission of secondary ions from outside of the central ~15 x 15 µm the measurement crater. The energy bandwidth for the secondary ions was ~50 eV. A mass resolving power > 5500 was used to separate interfering masses, such as $^{17}O^+$ from $^{16}OH^+$. Each measurement consisted of 120 seconds of presputtering, automatic secondary beam centering, and automatic mass calibration, followed by five cycles of counting of each ion intensity on an ETP electron multiplier in magnet peak jumping mode. Count times in seconds for each mass were as follows: $^{12}C^+ = 5$, $^{16}O^+ = 3$, $^{16}OH^+ = 5$, $^{19}F^+ = 5$, $^{30}Si^- = 2$, $^{31}P^+ = 5$, $^{32}S^+ = 5$, $^{35}Cl^+ = 5$. Background intensities were measured on Suprasil 3002 glass for C, OH, F, P, and S, and on Herasil glass for Cl.

f) Secondary Ion Mass Spectrometry at Caltech

Volatile concentration analyses were conducted on a Cameca ims-7f GEO instrument at the Caltech Microanalysis Center on the second indium mount. The standards were first measured with a Cs^+ beam, and later with an $^{16}O^-$ beam.

Cs SIMS measurements:

A 10 kV Cs+ primary ion beam of ~3-4 nA (~15 um in diameter) was used to sputter the samples and produce secondary ions. The beam was rastered to produce craters ~25 × 25 μm in dimension, and a 100 μm field aperture was used to enable only the ions from the central 8 μm of the craters to be transmitted for detection. Possible edge effects were further eliminated with electronic gating (36% in area). Secondary ions (^{12}C-, ^{16}OH-, ^{18}O-, ^{19}F-, ^{30}Si-, ^{31}P-, ^{32}S- and ^{35}Cl-) of -9 keV were collected with an electron multiplier (EM) in the peak-jumping mode. Each measurement consisted of 120 sec pre-sputtering, followed by automated secondary beam alignment, peak centering, and 20 cycles of data collection. The counting time of each mass was 1 sec per cycle. The energy bandwidth for the secondary ions was set at ~45 eV. Sample charging compensation was provided by a normal-incidence electron gun （NEG） at -10 kV. A mass resolving power (MRP) of ~5000 was used to remove any significant interferences to the masses of interest (e.g., ^{17}O- from the ^{16}OH- peak). Data were corrected for EM background and deadtime. The instrumental volatile backgrounds were checked with the Suprasil 3002 glass.

O^- SIMS measurements:

For this SIMS setup, a focused $^{16}O^-$ primary beam of -13 kV and ~8 nA was used to sputter areas of 25 x 25 um for analysis. Positive secondary ions of ^{1}H+, ^{12}C+, and ^{28}Si+ of +8.5 kV were collected in the peak-jumping mode with an EM (for ^{1}H+, ^{12}C+) or a Faraday cup (FC, for ^{28}Si+). Each measurement consisted of 20 cycles of counting of ^{1}H+(1s), ^{12}C+(3s), and ^{28}Si+ (1s). Because there were no significant interferences to the masses of interest, the mass spectrometer was operated at low mass resolution conditions (MRP ~1800). Minimal sample charging was corrected with automatic scan and adjustment of the sample high voltage during measurement. The other analytical parameters and operation were similar to those used for the Cs+ session.

g) Electron Microprobe at Caltech

Carbon contents of the glass samples ND70-3-01, ND70-4-02, ND70-5-02, and ND70-6-02 as well as the following secondary standards: five gem-quality scapolites (from Prof. George Rossman), a natural spurrite (from the Caltech mineral collection; CIT-11435; Joesten, 1974), and a eutectic glass composition in the CaO-Al_2O_3-SiO_2 (CAS) system were analyzed at Caltech using a JEOL JXA-iHP200F field-emission electron microprobe in WDS mode, interfaced with the Probe for EPMA software from Probe Software, Inc. The secondary

standards were carefully polished down to a ¼ μm finish and ultrasonicated in ethanol (the ND-series glasses were prepared at Lamont). Just prior to the start of the analytical session, the ND-series glasses, secondary standards, and primary standards were plasma cleaned using an Evactron system to remove hydrocarbon contamination on their surfaces and then coated with an ~1-nm layer of Ir (Armstrong & Crispin, 2013) using a Cressington 208HR sputter coater (all samples were coated at the same time). Analytical conditions were 10 kV and 15 kV accelerating voltages, a 50 nA beam current, and a 10 μm defocused beam. The LDE2 crystal was used for carbon analysis and counting times were 60 s on peak and 30 s on each background. The on-peak O interference with the C peak, revealed by WDS scans of the glass samples, was corrected using the Probe for EPMA program. Cohenite (Fe_3C; C$K\alpha$) from the iron meteorite Canyon Diablo and Elba hematite (O$K\alpha$; for the C on-peak interference correction) were used as primary standards. Each ND-series glass and secondary standard was analyzed five times. Quantitative carbon analyses were processed with the CITZAF matrix correction procedure (Armstrong, 1995) using the major and minor element composition of each phase.

For the secondary standards, the CO_2 contents of the five gem-quality scapolites were determined using NRA at the Michigan Ion Beam Laboratory at the University of Michigan using a deuteron beam energy of 1.35 MeV and following procedures described in Hammerli et al. (2021). The measured CO_2 contents ranged from 0.70 to 3.57 wt.%. The CAS eutectic glass was fused at 1-atm in air and is assumed to have a CO_2 content of zero (the extremely low solubility of CO_2 in basalts and more silica-rich compositions at pCO_2 = 1 bar, and the very low mole fraction of CO_2 in air support this assumption (e.g., Blank, 1993; Stolper & Holloway, 1988). Given spurrite's simple mineral chemistry, its CO_2 content is based on stoichiometry (abundant small inclusions on the surface of the polished sample precluded determining its C content by NRA).

Supplemental Figure S3 compares the measured EMP CO_2 contents of the secondary standards with their accepted values and shows that the probe analyses are systematically low and offset from the solid 1:1 line. The dashed line, an unweighted least-squares fit to the seven secondary standards, has an R^2-value of 0.997. We assumed that the EMP carbon analyses for the ND-series glasses were similarly offset from their "true" values, and we used the dashed-best-fit

line to adjust their CO_2 contents, i.e., to project them onto the y-axis in Fig. S3. It is these projected ND-series CO_2 concentrations that are plotted in Figure 2 and listed in Table 4.

h) Electron Microprobe at AMNH

The S, Cl and major element compositions were measured with a Cameca SX5-Tactis at the American Museum of Natural History. We used an accelerating voltage of 15 kV, a defocused beam of 10 µm, a beam current of 4 nA for Na (with 10s count time), 10 nA for Mg, Al, Si, Ca (20s count time), P, K, Ti, Mn, Fe (30s count time), and 40 nA for S and Cl (70s and 40s count times respectively). Na was analysed first to minimize Na loss during analysis. The instrument was calibrated on natural and synthetic mineral standards and glasses: albite (Na), olivine (Mg), potassium-feldspar (Al, Si and K), berlinite (P), anorthite (Ca), rutile (Ti), rhodonite (Mn), fayalite (Fe), barium sulfate (S) and scapolite (Cl). Errors (two standard deviation) are ±0.43 for SiO_2, ±0.18 for Na_2O, ±0.02 for K_2O, ±0.17 for Al_2O_3, ±0.36 for CaO, ±0.24 for FeO, ±0.11 for MgO, ±0.04 for TiO_2, ±0.05 for MnO, ±0.04 for P_2O_5, ±0.01 for S and ±0.03 for Cl.

IV. RESULTS

Here we compare results of the different analytical methods against the concentrations calculated from the quantities loaded into the experimental capsules. Loaded concentrations are used as a starting point for comparisons with no assumption that they might represent "correct" values. Results from EMPA analyses are given in table 3, results from ERDA, NRA, FTIR and EA are given in table 4 and results from SIMS are given in table 5. Raw SIMS results are given in tables S3 to S7. SIMS calibration lines are shown in figure S2 and S3. FTIR spectra and deconvolutions are shown in figure S5. Raw FTIR spectra are given in Moussallam (2024a). Raw NRA spectra are given in Moussallam (2024b).

a) H_2O

Water in the new reference glasses was analysed by ERDA, FTIR and at the ion microprobe facilities at CRPG-CNRS-Nancy, WHOI and Caltech. Figure 1 compares the water contents measured by all of these techniques with the expected (i.e., loaded) values. The agreement is in most cases excellent (better than 8%). Significant deviation from the one-to-one lines is only found for one Caltech Cs^+ beam SIMS analysis of sample ND70-4-02 although the discrepancy between loaded and measure H_2O content in ND70-4-02 disappears if the measured $^{16}O^1H/^{18}O$ ratio is used instead of the $^{16}O^1H/^{30}Si$ ratio. Caltech O^- beam SIMS analyses are not shown as most unknown glasses had values outside the calibration range for that session.

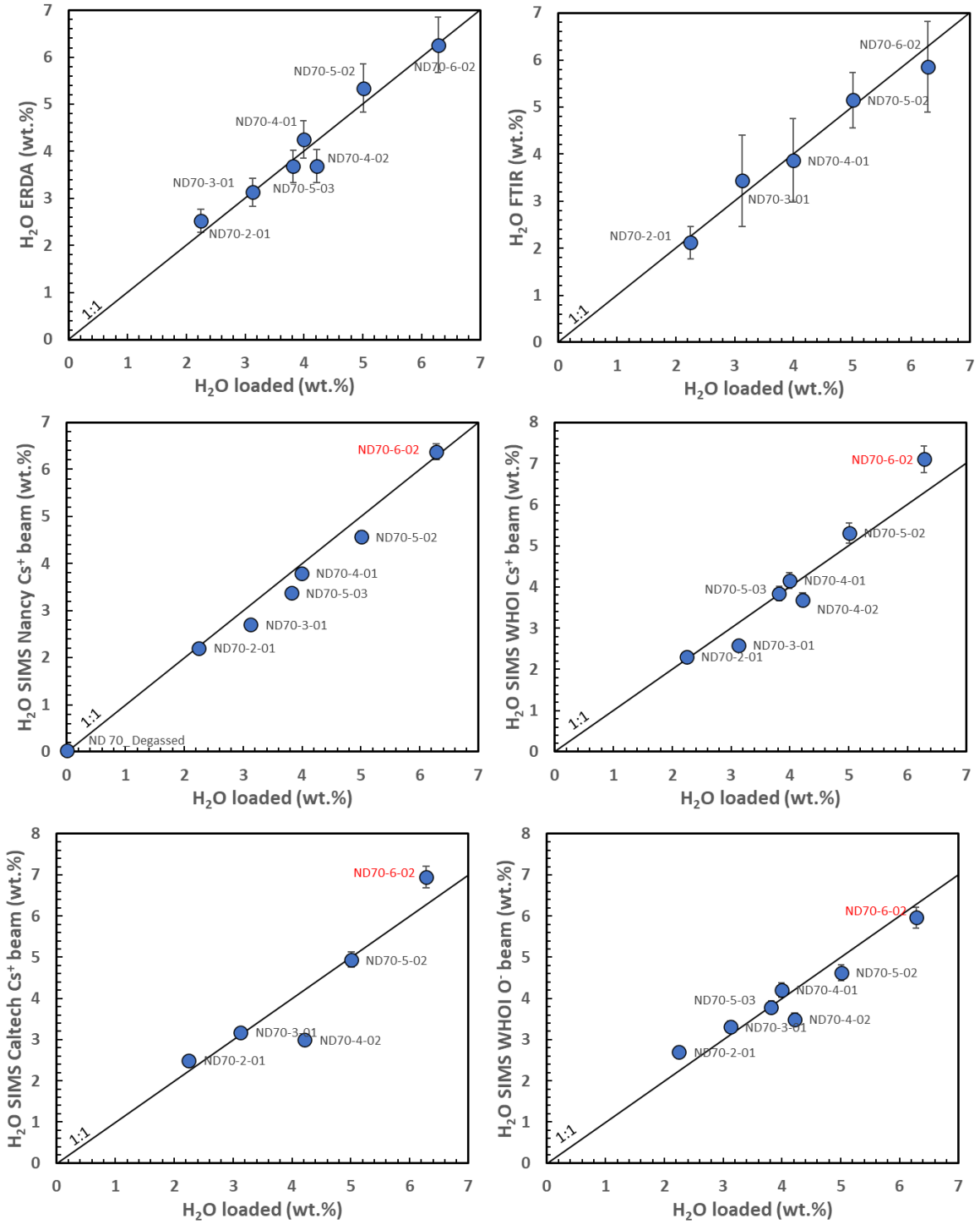

***Figure 1**: Comparison between the expected (i.e., loaded) and measured water content in the new reference materials. Samples labelled in red were measured outside calibration range.*

b) Carbon dioxide

CO_2 in the new reference glasses was analysed by NRA, EA, FTIR, EMPA and at the ion microprobe facilities at CRPG-CNRS-Nancy, WHOI and Caltech. Figure 2 compares the CO_2

355 contents measured by all these techniques with the expected (i.e., loaded) values. Sample
356 ND70_Degassed was only measured by SIMS (CRPG-CNRS-Nancy) which confirmed its
357 status as a "blank" (with CO_2 concentrations below the detection limit of ~100 ppm). Figure 2
358 shows that samples ND70-2-01, ND70-3-01, ND70-4-01, ND70-4-02 and ND70-5-03 have
359 measured CO_2 contents significantly higher than expected based on the loaded amounts of CO_2
360 (although not all five samples were analysed using all of the techniques or ion probes). Samples
361 ND70-5-02 measured CO_2 contents were significantly higher expected from than loaded values
362 from NRA, and EA analyses, close to expected in EMPA and O^- beam SIMS analyses from
363 Caltech and WHOI and significantly lower than expected in Cs^+ beam SIMS analyses at CRPG-
364 CNRS-Nancy, WHOI and Caltech. Samples ND70-6-02 measured CO_2 contents were
365 significantly higher than expected in NRA analyses, close to expected in EA and FTIR analyses
366 and significantly lower than expected in EMPA and all SIMS analyses across facilities and
367 primary beam conditions.

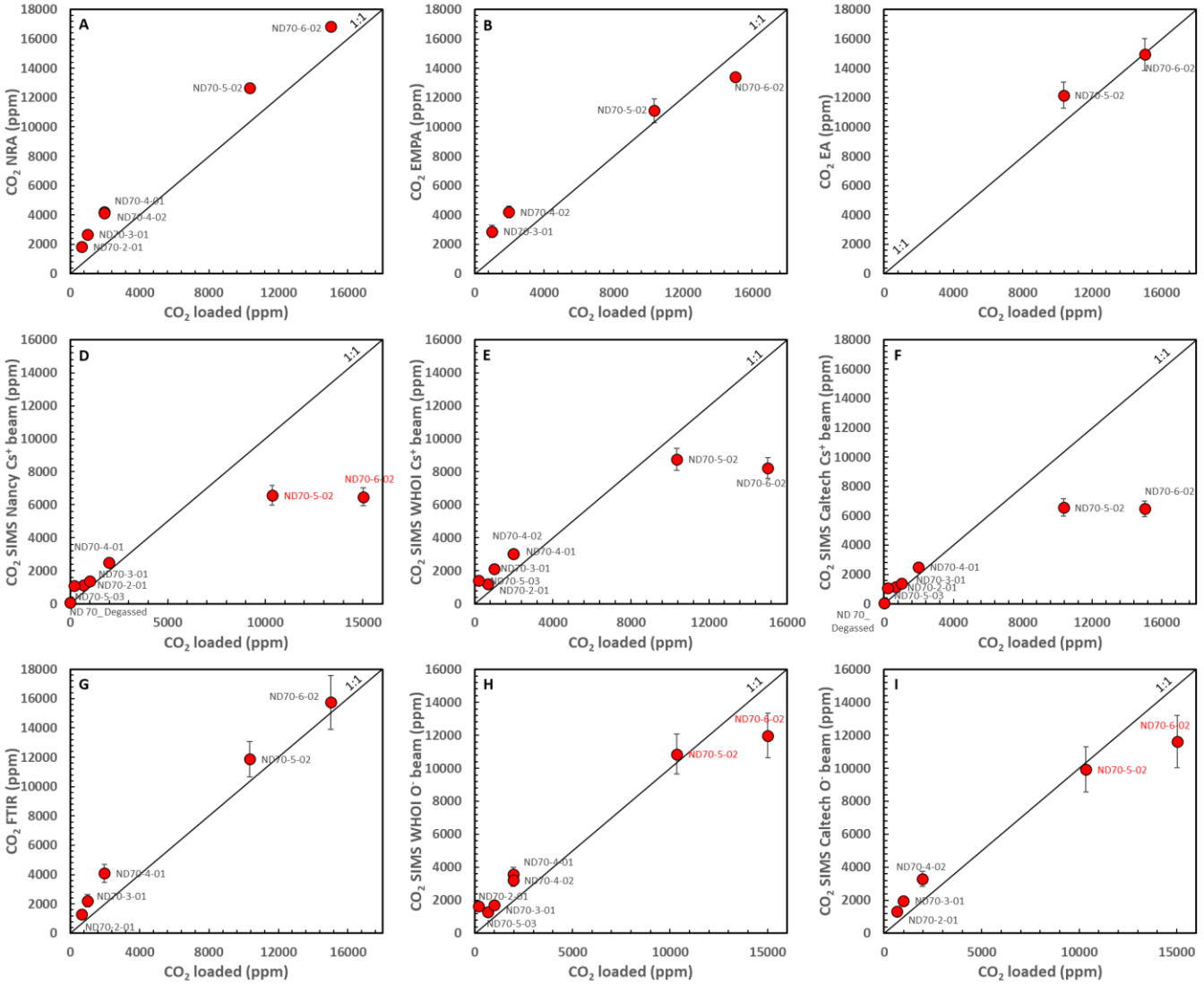

Figure 2*: Comparison between the expected (i.e., loaded) and measured CO_2 content in the new reference materials. Samples labelled in red were measured outside calibration range.*

c) Sulphur

S in the new reference glasses was analysed by EMP at AMNH and at the ion microprobe facilities at CRPG-CNRS-Nancy, WHOI and Caltech. Figure 3 compares the loaded S contents with the concentrations measured by EMP and the three ion probes. The agreement is excellent for samples ND70_Degassed, ND70-2-01, ND70-3-01, ND70-5-03 and ND70-5-02. Samples ND70-4-01 and ND70-4-02 show somewhat lower than expected values in the Caltech and WHOI SIMS analyses. The measured S contents in sample ND70-6-02 were significantly lower than the loaded concentrations in the EMP and Caltech and WHOI SIMS analyses and higher than expected in the Nancy SIMS analyses. Note that the SIMS S measurements for both ND70-5-02 and ND70-6-02 are based on very significant extrapolation from calibration ranges (Figure S2).

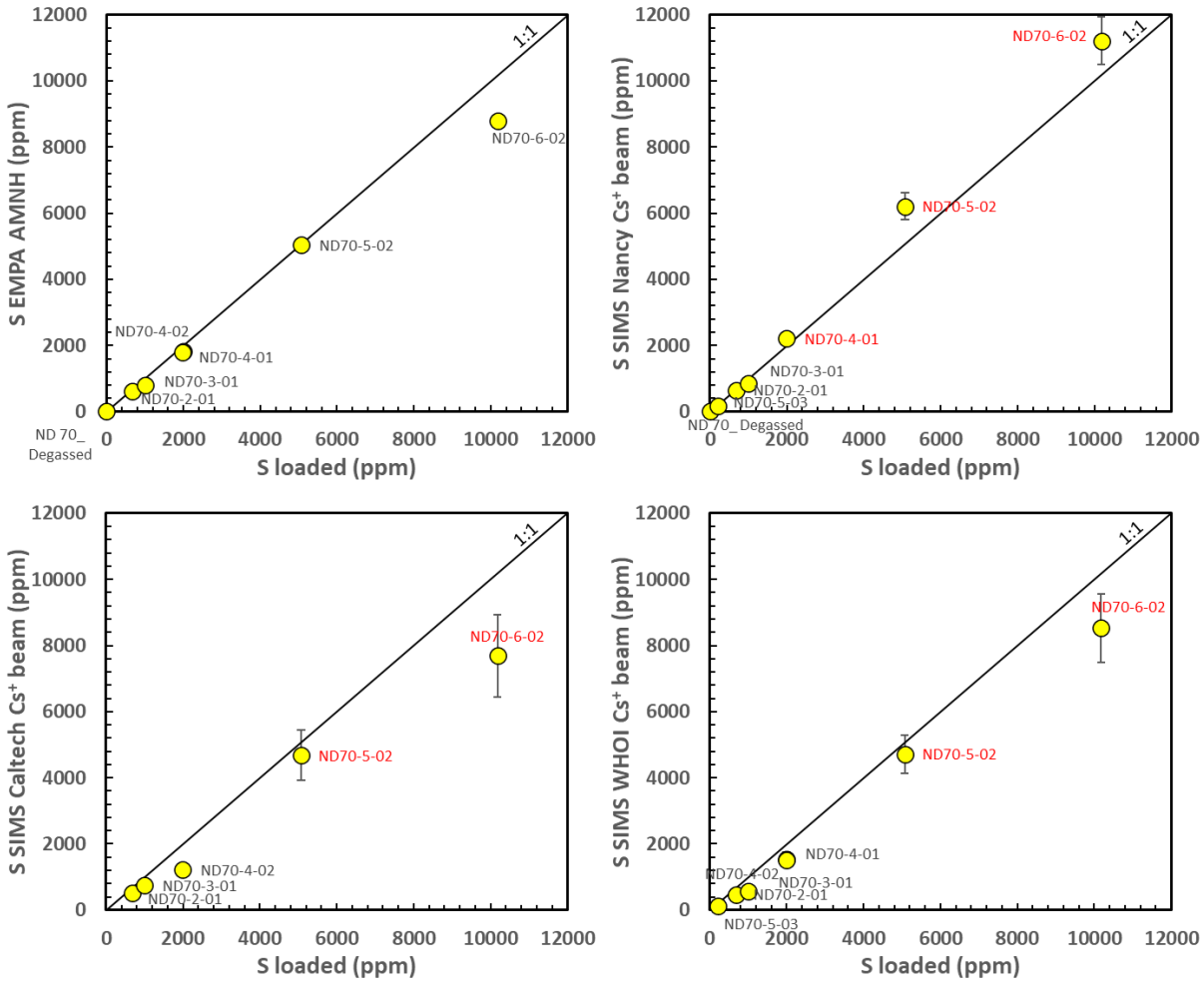

***Figure 3**: Comparison between the expected (i.e., loaded) and measured S content in the new reference materials. Samples labelled in red were measured outside calibration range.*

d) Chlorine

Chlorine in the new reference glasses was analysed by EMP at AMNH and at the ion microprobe facilities at CRPG-CNRS-Nancy, WHOI and Caltech (the Caltech analyses are not shown as most of the unknown glasses had values outside the calibration range for that session). Figure 4 compares the Cl contents measured by these techniques with the expected (i.e., loaded) values. Samples ND70_Degassed, ND70-2-01, ND70-3-01, ND70-4-01, ND70-4-02 and ND70-5-03 all show good to excellent agreements. The measured Cl contents in samples ND70-5-02 and ND70-6-02 are significantly higher than expected from loaded amounts in both sets of SIMS analyses and in the EMP analyses. Note that the SIMS Cl measurements for both ND70-5-02 and ND70-6-02 are based on very significant extrapolation from calibration ranges (Figure S2).

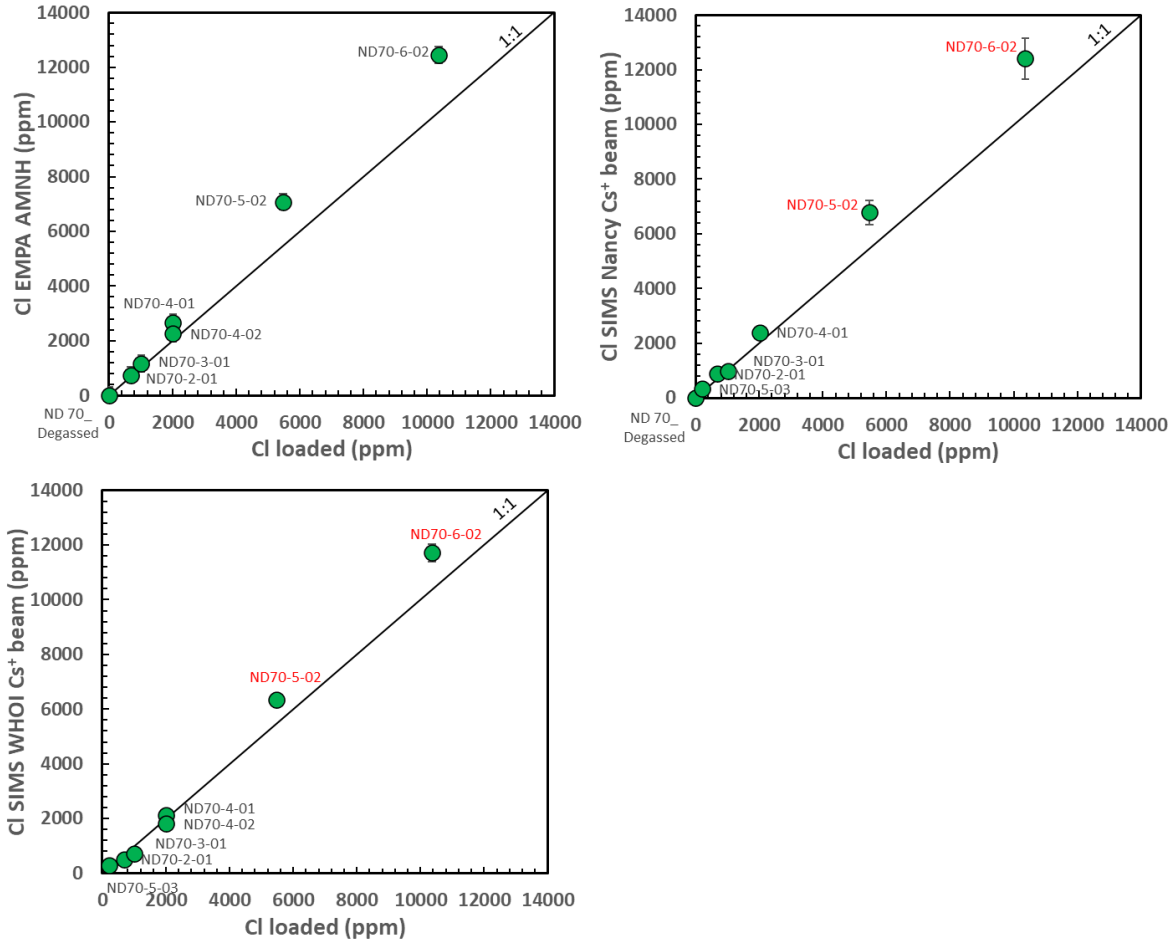

***Figure 4**: Comparison between the expected (i.e., loaded) and measured Cl content in the new reference materials. Samples labelled in red were measured outside calibration range.*

e) Fluorine

Fluorine in the new reference glasses was analysed at the ion microprobe facilities at CRPG-CNRS-Nancy, WHOI and Caltech but Caltech analyses are not shown as most of the unknown

glasses had F concentrations outside the calibration range for that session. Figure 5 compares the F contents measured by the Nancy and WHOI ion probes with the expected (i.e., loaded) values; all samples show excellent agreement between the measured and expected concentrations (even for samples ND70-5-02 and ND70-6-02 where measurements are based on very significant extrapolation from calibration ranges; Figure S2).

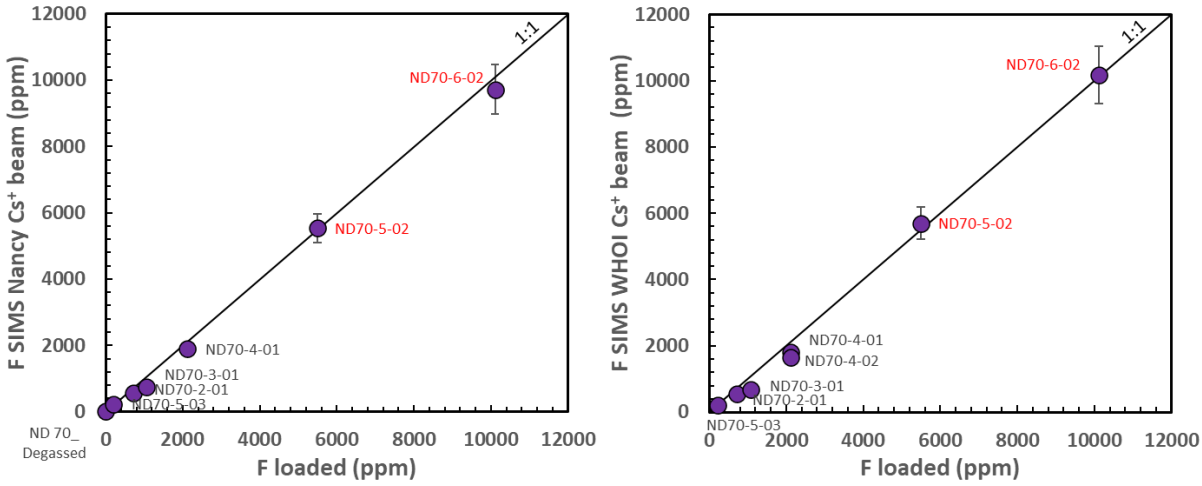

Figure 5*: Comparison between the expected (i.e., loaded) and measured F content in the new reference materials. Samples labelled in red were measured outside calibration range.*

V. DISCUSSION

a) Inter-instrument comparison

Figure 6 compares the mean absolute deviation (in %) between all the techniques used to measure H_2O, CO_2, S, Cl and F contents in the ND70 suite, and figure 7 graphically compares the measurements. For H_2O, results from ERDA, FTIR and four SIMS sessions all agree very well with average mean absolute deviations around 10% between methods. For CO_2, NRA, EA, FTIR and EMPA analyses are in good agreement with each other (on average within ±9%). Cs^+ primary beam SIMS analyses at Caltech, WHOI and Nancy agree reasonably well with each other (on average within ±18%) but agree poorly with other techniques due to samples ND70-5-02 and ND70-6-02, outside the calibration range for the Nancy SIMS session and dominating the mean absolute deviation (more on this in the following section). O^- primary beam SIMS analyses at Caltech and WHOI are in good agreement (within ±6%), in reasonable agreement with the results from NRA, EA and FTIR (on average within ±19%), and differ from the EMPA concentrations by, on average, ±27%. Note that only two samples were analysed by EA, possibly explaining why this technique shows the lowest average mean absolute deviation.

For S, the averages of the EMP analyses and the three sets of Cs^+ primary beam SIMS analyses (Caltech, WHOI and Nancy) all agree within approximately ±20%; the average deviation between these four sets of average S contents and the loaded amounts is also ~ 20% (despite several samples, ND70-5-02, ND70-6-02 and for the Nancy session, ND70-4-01, being outside the calibration range for the SIMS analyses). For Cl, the means of the EMP analyses and the two sets of Cs^+ primary beam SIMS analyses (WHOI and Nancy) all agree, on average, within ±19%; the agreement is similar when the means are compared to the loaded amounts of Cl despite samples ND70-5-02 and ND70-6-02 being outside the calibration range for the SIMS analyses. The EMPA and Nancy SIMS analyses agree within ±10%. The means of the two sets of Cs^+ primary beam F SIMS analyses (WHOI and Nancy) agree, on average, within ±10%. The loaded amounts of F agree with the SIMS averages to within ~13%, despite samples ND70-5-02 and ND70-6-02 being outside the calibration range for both SIMS sessions.

H_2O	ERDA	FTIR	SIMS Cs+ Caltech	SIMS Cs+ WHOI	SIMS O- WHOI	SIMS Cs+ Nancy		Average*
Loaded	6	6	11	8	9	7		8
ERDA		8	8	7	6	10		8
FTIR			13	13	10	10		10
SIMS Cs+ Caltech				12	10	11		11
SIMS Cs+ WHOI					12	9		10
SIMS O- WHOI						11		10
SIMS Cs+ Nancy								10

CO_2	NRA	EA	FTIR	SIMS Cs+ Caltech	SIMS O- Caltech	SIMS Cs+ WHOI	SIMS O- WHOI	SIMS Cs+ Nancy	EMPA		Average*
Loaded	101	9	70	48	59	140	155	115	81		86
NRA		8	12	42	25	32	24	47	11		34
EA			3	42	20	36	15	51	9		22
FTIR				28	15	22	14	38	16		24
SIMS Cs+ Caltech					33	17	35	14	71		37
SIMS O- Caltech						13	6	31	25		25
SIMS Cs+ WHOI							20	21	41		38
SIMS O- WHOI								30	28		36
SIMS Cs+ Nancy									94		49
EMPA											42

S	EMPA AMNH	SIMS Cs+ Caltech	SIMS Cs+ WHOI	SIMS Cs+ Nancy		Average*
Loaded	10	24	25	12		18
EMPA AMNH		16	15	15		14
SIMS Cs+ Caltech			13	30		21
SIMS Cs+ WHOI				38		23
SIMS Cs+ Nancy						24

Cl	Loaded	EMPA AMNH	SIMS Cs+ WHOI	SIMS Cs+ Nancy		Average*
Loaded		20	21	19		20
EMPA AMNH			21	10		17
SIMS Cs+ WHOI				24		22
SIMS Cs+ Nancy						17

F	Loaded	SIMS Cs+ WHOI	SIMS Cs+ Nancy		Average*
Loaded		15	12		13
SIMS Cs+ WHOI			5		10
SIMS Cs+ Nancy					9

*Average of mean absolute deviation across methods (in %)

Figure 6: *Matrices showing the mean absolute deviation (in %) between all techniques used to measure H_2O, CO_2, S, Cl and F contents in the new reference materials. Background boxes colours are scaled with the mean absolute deviation from green to red.*

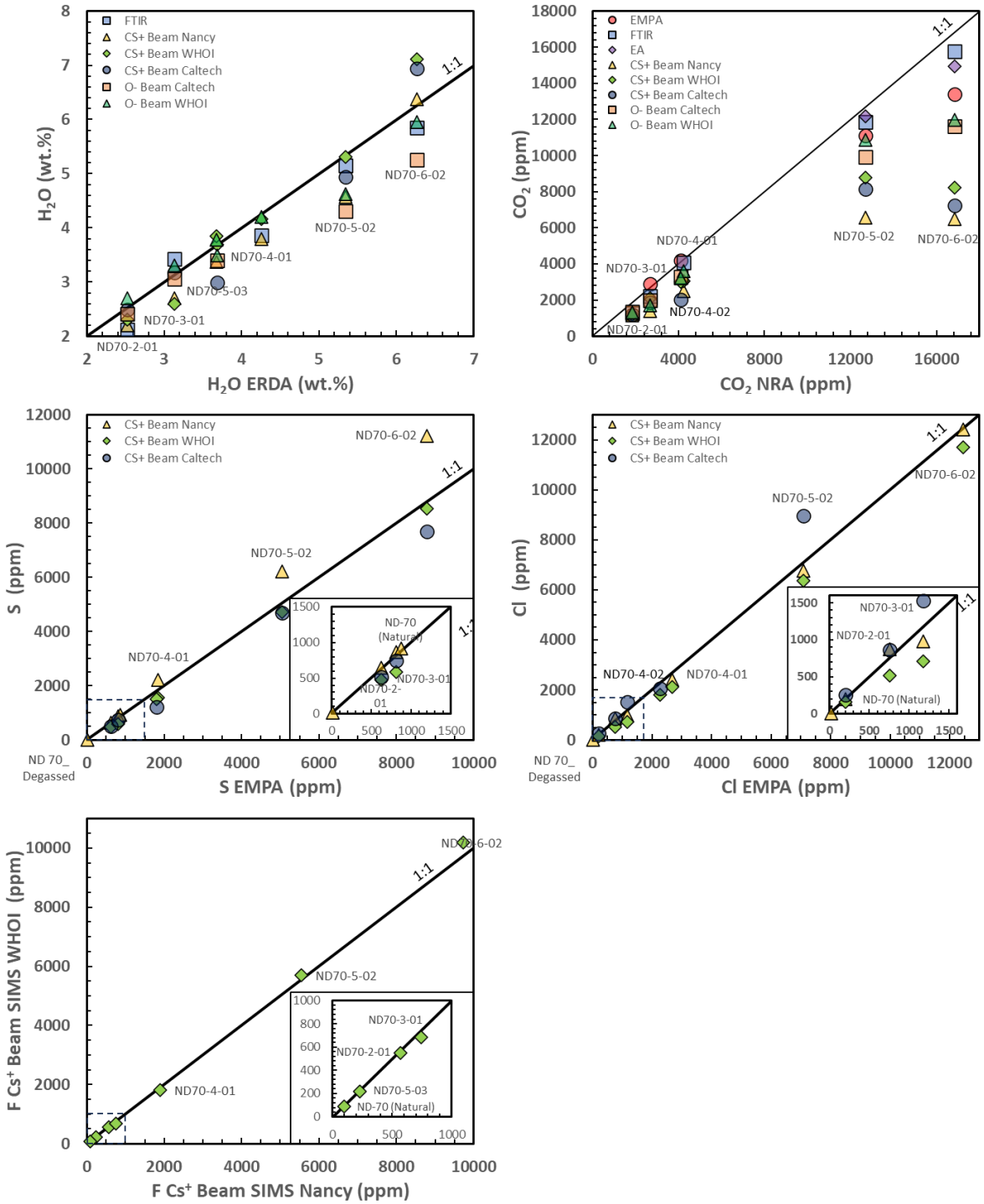

***Figure** 7: Comparison of measured H_2O, CO_2, S, Cl and F volatile content in ND70-series glasses by several techniques.*

b) Effect of water on SIMS CO_2 measurements

All three Cs^+ primary beam SIMS sessions (Caltech, WHOI and Nancy), yielded CO_2 contents for ND70-5-02 and, especially ND70-6-02, that were low relative to the loaded abundances of CO_2. The loaded CO_2 abundance in sample ND70-6-02 was 1.5 wt.% (verified by FTIR, EA and NRA), yet the Cs^+ primary beam SIMS analyses at all three ion probes measured $^{12}C/^{30}Si$ ratios much lower than expected for such concentrations (see Figure S2). In all three cases, the measured $^{12}C/^{30}Si$ ratios were even lower than the ones measured in sample ND70-5-02 which contained 1 wt.% CO_2. We attribute this anomaly to the high water concentration of ND70-6-02 (> 6 wt%), limiting the ionization efficiency of ^{12}C, a phenomenon previously reported in an AGU abstract by Hervig et al. (2009). Figure 8 shows the ionization efficiency ratios, $(^{12}C/^{30}Si \times SiO_2)/CO_2$ and $(^{12}C/^{18}O \times SiO_2)/CO_2$, as a function of the water content in all the glasses analysed during all SIMS sessions. If water had no effect on the ^{12}C ion probe signal, both ratios should remain constant as a function of water content. What we observe, however, is that these ratios vary greatly. At low (<2 wt.%) water contents, the ratios are quite variable; in the Caltech and WHOI SIMS sessions, there is a hint of a possible positive correlation between C ionization efficiency and the glass water content, peaking at ~1.5 wt.% H_2O. At high (>2 wt.%) water contents, the C ionization efficiency seems to become more stable, at least in the explored range (2.5 to 6 wt.% H_2O), although there is still a hint of an inverse correlation between water content and C ionization efficiency (Figure 8A and B). The ~2 wt.% cut-off between the two behaviours could be related to water speciation in the glass. In silicate glass, water dissolves mainly as hydroxyl groups at low water concentrations, whereas at higher concentrations it dissolves primarily as molecular water (e.g, Stolper, 1982). At around 2 wt.% total water, the rate at which the hydroxyl group concentration increases begins to slow, while the rate at which the molecular water concentration increases accelerates. The fact that the C ionisation efficiency is so variable between SIMS sessions suggests that the magnitude of the effect may be related to beam conditions.

Although Hervig et al. (2009) reported that using an O^- primary beam significantly mitigates the influence of H_2O on the carbon ion yield, we found that O^- primary beam analyses also suffered from the same effect (Figure 8 C and D; note that the magnitude of the effect, although based on a smaller number of analyses, may potentially be less), The consequences of this C ionization efficiency reduction for SIMS carbon analyses are potentially dire. For example, if one were to analyse carbon in a natural basaltic glass containing 4 wt.% water using a Cs^+ primary beam and glass standards with less than 2 wt.% water, the unknown CO_2

concentrations could be underestimated by two to three-fold. The corollary is also true, using standards with high water contents to measure CO_2 concentrations in samples with low water content will result in large overestimations. It is likely that these effects permeate the literature of published glass and melt inclusion CO_2 concentration data. Thus, to accurately measure CO_2 by SIMS, one needs to select reference materials with water concentrations matching that of the unknown sample or to characterise the signal dependency on water concentration as in Figure 8.

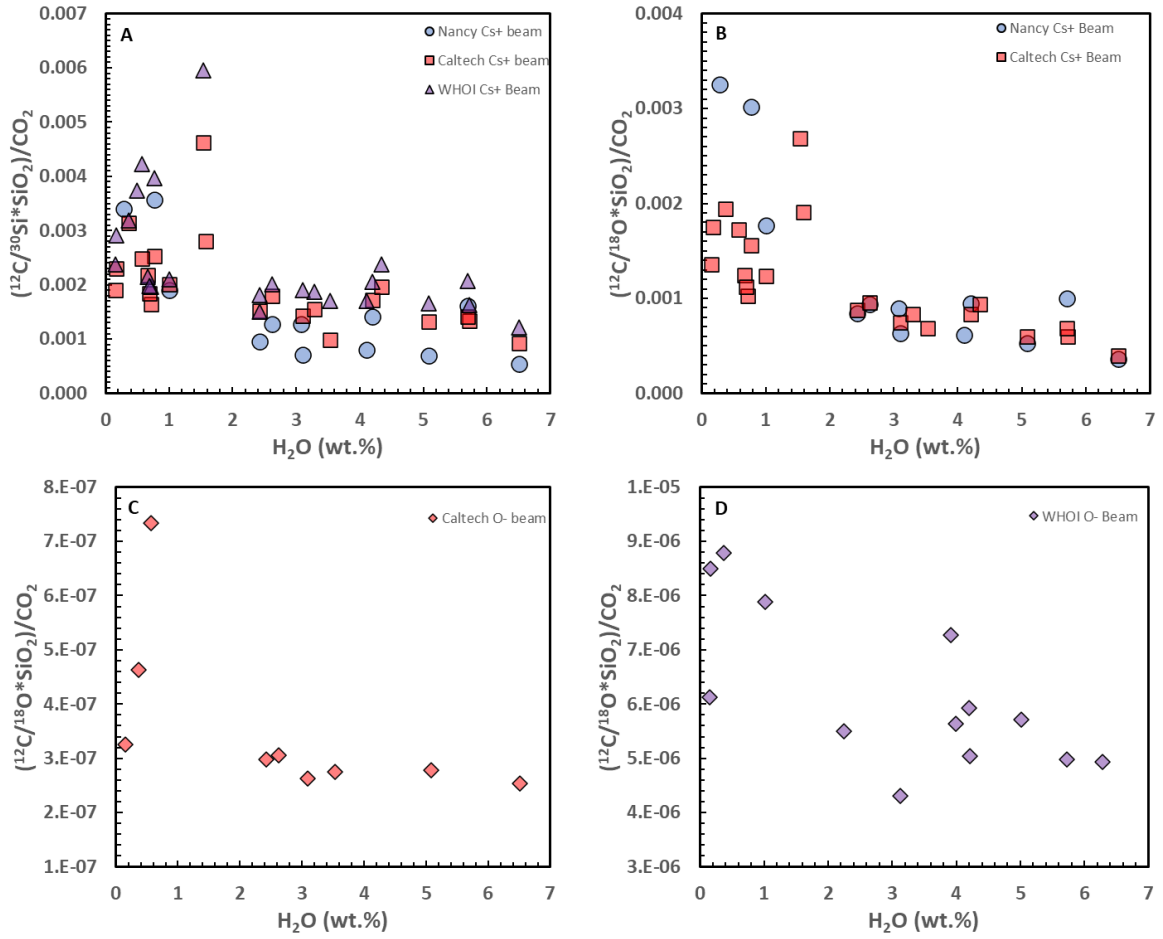

Figure 8: *Effect of water on the ($^{12}C/^{30}Si \times SiO_2$)/$CO_2$ and ($^{12}C/^{18}O \times SiO_2$)/$CO_2$ ratios measured by SIMS (i.e., the calibration line). The results of three SIMS sessions using a Cs^+ primary beam and two SIMS sessions using a O^- primary beam are reported. In all cases the glass water content seems to greatly reduce the ionization efficiency of ^{12}C.*

499 **c) Final compositions of the new reference materials**

500 The compositions of the new reference materials we see as the most accurate, and which we
501 encourage researchers to use in future studies are reported in table 6. For H_2O, since all
502 techniques closely agree within 13% (Fig. 6), we used the average values from ERDA, FTIR,
503 the three Cs^+ primary beam SIMS sessions at Caltech, WHOI and Nancy, the O^- primary beam
504 session at WHOI and report the uncertainty as the standard deviation from these averages. For
505 CO_2, given the strong effect of water on suppressing C ionization efficiency (see previous
506 section), we used the average of the NRA, EA and FTIR analyses and, for the low C (<5000
507 ppm) samples, we also included the EMP analyses. We report the uncertainty as the standard
508 deviation from these averages. For ND70_Natural we report the average of all SIMS and FTIR
509 sessions along with the associated standard deviation. For S, since all techniques agreed
510 closely, we used the average values from EMPA and the three Cs^+ primary beam SIMS sessions
511 (Caltech, WHOI and Nancy) and report the uncertainty as the standard deviation from these
512 averages. For Cl, we used the average values from EMPA and two Cs^+ primary beam SIMS
513 sessions at WHOI and Nancy and report the uncertainty as the standard deviation from these
514 averages. For F, we used the average values from two Cs^+ primary beam SIMS sessions at
515 WHOI and Nancy and report the uncertainty as the standard deviation from these averages.
516

517 # VI. CONCLUSION
518

519 We present a new set of reference materials designed for in situ analysis of volatile elements
520 (H_2O, CO_2, S, Cl, F) in basaltic silicate glass. The starting material was fused in air and splits
521 with variable amounts of volatiles were subsequently run in the piston cylinder. The resulting
522 reference glasses (the ND-70 series) span a wide range of concentrations from 0 to 6 wt.%
523 H_2O, 0 to 1.6 wt.% CO_2, and 0 to 1 wt.% S, Cl and F. The samples were characterized by
524 Elastic Recoil Detection Analysis, Nuclear Reaction Analysis, Elemental Analyser, Fourier
525 Transform Infrared Spectroscopy, Secondary Ion Mass Spectrometry, and Electron
526 Microprobe.
527

528 Most analytical techniques provided good agreement with the expected volatile concentrations
529 in each of the glasses; agreement between techniques and between different ion probes is also
530 generally good. CO_2 measurements are the exception and deviated significantly from expected
531 values across analytical methods; however, inter-method reproducibility was good except for

SIMS measurements. We found that this discrepancy was likely due to the samples' high-water contents, which have a substantial impact on the ionization efficiency of ^{12}C during SIMS analyses. This underscores the importance of carefully selecting reference materials with water concentrations matching those of unknown samples or characterizing the signal dependency on water content to ensure accurate CO_2 measurements by SIMS.

The reference materials we have presented in this study offer a community resource for the analysis of volatile elements in basaltic silicate glass, particularly when using SIMS and other micro-beam techniques. These materials are being made available at various ion probe facilities and at the Smithsonian National Museum of Natural History where they will be freely available on loan (a catalogue numbers will be available for the final manuscript version). We encourage researchers to utilize them to improve the accuracy and inter-laboratory comparability of their measurements.

DATA AVAILABILITY STATEMENT

Raw FTIR spectra are archived as Moussallam (2024a). Raw NRA spectra are archived as Moussallam (2024b).

ACKNOWLEDGEMENTS

We thank Nordine Bouden and Johan Villeneuve for their invaluable support during the ion probe analyses at CNRS-CRPG-Nancy.

AUTHOR CONTRIBUTIONS

Initial study design: W.H.T., Y.M., T.P.

Experiments: W.H.T., Y.M., S.D.

ERDA: H.B., H.K.

NRA: H.B., H.K.

EA: H.L.

FTIR: S.D., H.L., S.S.

SIMS (Nancy): Y.M., E.R.K.

SIMS (WHOI): B.M., G.G.,

SIMS (Caltech): T.P., Y.G.

EMPA (Caltech): E.M.S., M.B., C.M.

EMPA (AMNH): Y.M., S.D., W.H.T.

Writing and interpretation: All authors, first draft Y.M.

564

565

566 **REFERENCES**

567 Albarède, F. (2009). Volatile accretion history of the terrestrial planets and dynamic
568 implications. *Nature*, *461*(7268), 1227–1233. https://doi.org/10.1038/nature08477
569 Allard, P. (2010). A CO2-rich gas trigger of explosive paroxysms at Stromboli basaltic
570 volcano, Italy. *Journal of Volcanology and Geothermal Research*, *189*(3–4), 363–374.
571 https://doi.org/10.1016/j.jvolgeores.2009.11.018
572 Armstrong, J. (1995). CITZAF: a package of correction programs for the quantitative electron
573 microbeam X-ray-analysis of thick polished materials, thin films, and particles.
574 *Microbeam Analysis*, *4*, 177.
575 Armstrong, J., & Crispin, K. (2013). Ultra-thin Iridium as a Replacement Coating for Carbon
576 in High Resolution Quantitative Analyses of Insulating Specimens. *Microscopy and*
577 *Microanalysis*, *19*(S2), 1070–1071. https://doi.org/10.1017/S1431927613007344
578 Blank, J. G. (1993). *An experimental investigation of the behavior of carbon dioxide in rhyolitic*
579 *melt* (phd). California Institute of Technology. https://doi.org/10.7907/tq3x-2059
580 Bureau, H., Raepsaet, C., Khodja, H., Carraro, A., & Aubaud, C. (2009). Determination of
581 hydrogen content in geological samples using elastic recoil detection analysis (ERDA).
582 *Geochimica et Cosmochimica Acta*, *73*(11), 3311–3322.
583 https://doi.org/10.1016/j.gca.2009.03.009
584 Caulfield, J., Turner, S., Arculus, R., Dale, C., Jenner, F., Pearce, J., et al. (2012). Mantle flow,
585 volatiles, slab-surface temperatures and melting dynamics in the north Tonga arc–Lau
586 back-arc basin. *Journal of Geophysical Research: Solid Earth*, *117*(B11).
587 https://doi.org/10.1029/2012JB009526
588 Clesi, V., Bouhifd, M. A., Bolfan-Casanova, N., Manthilake, G., Schiavi, F., Raepsaet, C., et
589 al. (2018). Low hydrogen contents in the cores of terrestrial planets. *Science Advances*,
590 *4*(3), e1701876. https://doi.org/10.1126/sciadv.1701876
591 Dasgupta, R., & Hirschmann, M. M. (2006). Melting in the Earth's deep upper mantle caused
592 by carbon dioxide. *Nature*, *440*(7084), 659–662. https://doi.org/10.1038/nature04612
593 Dehant, V., Debaille, V., Dobos, V., Gaillard, F., Gillmann, C., Goderis, S., et al. (2019).
594 Geoscience for Understanding Habitability in the Solar System and Beyond. *Space*
595 *Science Reviews*, *215*(6), 42. https://doi.org/10.1007/s11214-019-0608-8

596 Dixon, J. E., Stolper, E., & Delaney, J. R. (1988). Infrared spectroscopic measurements of CO2
597 and H2O in Juan de Fuca Ridge basaltic glasses. *Earth and Planetary Science Letters*,
598 *90*(1), 87–104. https://doi.org/10.1016/0012-821X(88)90114-8
599 Edmonds, M., & Woods, A. W. (2018). Exsolved volatiles in magma reservoirs. *Journal of*
600 *Volcanology and Geothermal Research*, *368*, 13–30.
601 https://doi.org/10.1016/j.jvolgeores.2018.10.018
602 Eggler, D. H. (1976). Does CO2 cause partial melting in the low-velocity layer of the mantle?
603 *Geology*, *4*(2), 69–72. https://doi.org/10.1130/0091-
604 7613(1976)4<69:DCCPMI>2.0.CO;2
605 Ehlmann, B. L., Anderson, F. S., Andrews-Hanna, J., Catling, D. C., Christensen, P. R., Cohen,
606 B. A., et al. (2016). The sustainability of habitability on terrestrial planets: Insights,
607 questions, and needed measurements from Mars for understanding the evolution of
608 Earth-like worlds. *Journal of Geophysical Research: Planets*, *121*(10), 1927–1961.
609 https://doi.org/10.1002/2016JE005134
610 Elskens, I., Tazieff, H., & Tonani, F. (1968). Investigations Nouvelles sur les Gaz Volcaniques.
611 *Bulletin Volcanologique*, *32*(3), 521–574. https://doi.org/10.1007/BF02599800
612 Foley, B. J., & Smye, A. J. (2018). Carbon Cycling and Habitability of Earth-Sized Stagnant
613 Lid Planets. *Astrobiology*, *18*(7), 873–896. https://doi.org/10.1089/ast.2017.1695
614 Hammerli, J., Hermann, J., Tollan, P., & Naab, F. (2021). Measuring in situ CO2 and H2O in
615 apatite via ATR-FTIR. *Contributions to Mineralogy and Petrology*, *176*(12), 105.
616 https://doi.org/10.1007/s00410-021-01858-6
617 Hauri, E., Wang, J., Dixon, J. E., King, P. L., Mandeville, C., & Newman, S. (2002). SIMS
618 analysis of volatiles in silicate glasses: 1. Calibration, matrix effects and comparisons
619 with FTIR. *Chemical Geology*, *183*(1–4), 99–114. https://doi.org/10.1016/S0009-
620 2541(01)00375-8
621 Hervig, R. L., Moore, G. M., & Roggensack, K. (2009). Calibrating Carbon Measurements in
622 Basaltic Glass Using SIMS and FTIR: The Effect of Variable H2O Contents, *2009*,
623 V51E-1755. Presented at the AGU Fall Meeting Abstracts.
624 Jarosewich, E., Nelen, J. a., & Norberg, J. A. (1980). Reference Samples for Electron
625 Microprobe Analysis*. *Geostandards Newsletter*, *4*(1), 43–47.
626 https://doi.org/10.1111/j.1751-908X.1980.tb00273.x
627 Jochum, K. P., Stoll, B., Herwig, K., Willbold, M., Hofmann, A. W., Amini, M., et al. (2006).
628 MPI-DING reference glasses for in situ microanalysis: New reference values for

element concentrations and isotope ratios. *Geochemistry, Geophysics, Geosystems*, *7*(2). https://doi.org/10.1029/2005GC001060

Kamenetsky, V. S., Everard, J. L., Crawford, A. J., Varne, R., Eggins, S. M., & Lanyon, R. (2000). Enriched End-member of Primitive MORB Melts: Petrology and Geochemistry of Glasses from Macquarie Island (SW Pacific). *Journal of Petrology*, *41*(3), 411–430. https://doi.org/10.1093/petrology/41.3.411

Keller, N. S., Arculus, R. J., Hermann, J., & Richards, S. (2008). Submarine back-arc lava with arc signature: Fonualei Spreading Center, northeast Lau Basin, Tonga. *Journal of Geophysical Research: Solid Earth*, *113*(B8). https://doi.org/10.1029/2007JB005451

Khodja, H., Berthoumieux, E., Daudin, L., & Gallien, J.-P. (2001). The Pierre Süe Laboratory nuclear microprobe as a multi-disciplinary analysis tool. *Nuclear Instruments and Methods in Physics Research Section B: Beam Interactions with Materials and Atoms*, *181*(1), 83–86. https://doi.org/10.1016/S0168-583X(01)00564-X

Lloyd, A. S., Plank, T., Ruprecht, P., Hauri, E. H., & Rose, W. (2013). Volatile loss from melt inclusions in pyroclasts of differing sizes. *Contributions to Mineralogy and Petrology*, *165*(1), 129–153. https://doi.org/10.1007/s00410-012-0800-2

Malavergne, V., Bureau, H., Raepsaet, C., Gaillard, F., Poncet, M., Surblé, S., et al. (2019). Experimental constraints on the fate of H and C during planetary core-mantle differentiation. Implications for the Earth. *Icarus*, *321*, 473–485. https://doi.org/10.1016/j.icarus.2018.11.027

Mayer, M. (1999). SIMNRA, a simulation program for the analysis of NRA, RBS and ERDA. *AIP Conference Proceedings*, *475*(1), 541–544. https://doi.org/10.1063/1.59188

Métrich, N., & Wallace, P. J. (2008). Volatile Abundances in Basaltic Magmas and Their Degassing Paths Tracked by Melt Inclusions. *Reviews in Mineralogy and Geochemistry*, *69*(1), 363–402. https://doi.org/10.2138/rmg.2008.69.10

Mosbah, M., Metrich, N., & Massiot, P. (1991). PIGME fluorine determination using a nuclear microprobe with application to glass inclusions. *Nuclear Instruments and Methods in Physics Research Section B: Beam Interactions with Materials and Atoms*, *58*(2), 227–231. https://doi.org/10.1016/0168-583X(91)95592-2

Moussallam, Y. (2024a). ND70 paper_Raw FTIR spectra [Data set]. figshare. https://doi.org/10.6084/m9.figshare.25292692.v1

Moussallam, Y. (2024b). ND70 paper_Raw NRA Spectra [Data set]. figshare. https://doi.org/10.6084/m9.figshare.25292674.v1

662 Moussallam, Y., Morizet, Y., Massuyeau, M., Laumonier, M., & Gaillard, F. (2015). CO2
663 solubility in kimberlite melts. *Chemical Geology*, *418*, 198–205.
664 https://doi.org/10.1016/j.chemgeo.2014.11.017
665 Moussallam, Y., Morizet, Y., & Gaillard, F. (2016). H2O–CO2 solubility in low SiO2-melts
666 and the unique mode of kimberlite degassing and emplacement. *Earth and Planetary*
667 *Science Letters*, *447*, 151–160. https://doi.org/10.1016/j.epsl.2016.04.037
668 Moussallam, Y., Lee, H. J., Ding, S., DeLessio, M., Everard, J. L., Spittle, E., et al. (2023).
669 Temperature of the Villarrica Lava Lake from 1963 to 2015 Constrained by Phase-
670 Equilibrium and a New Glass Geothermometer for Basaltic Andesites. *Journal of*
671 *Petrology*, *64*(2). https://doi.org/10.1093/petrology/egad003
672 Nicoli, G., & Ferrero, S. (2021). Nanorocks, volatiles and plate tectonics. *Geoscience*
673 *Frontiers*, *12*(5), 101188. https://doi.org/10.1016/j.gsf.2021.101188
674 Shimizu, K., Ushikubo, T., Hamada, M., Itoh, S., Higashi, Y., Takahashi, E., & Ito, M. (2017).
675 H_2O, CO_2, F, S, Cl, and P_2O_5 analyses of silicate glasses using SIMS: Report of volatile
676 standard glasses. *Geochemical Journal*, *51*(4), 299–313.
677 https://doi.org/10.2343/geochemj.2.0470
678 Shishkina, T. A., Botcharnikov, R. E., Holtz, F., Almeev, R. R., & Portnyagin, M. V. (2010).
679 Solubility of H2O- and CO2-bearing fluids in tholeiitic basalts at pressures up to
680 500 MPa. *Chemical Geology*, *277*(1–2), 115–125.
681 https://doi.org/10.1016/j.chemgeo.2010.07.014
682 Stern, R. J. (2018). The evolution of plate tectonics. *Philosophical Transactions of the Royal*
683 *Society A: Mathematical, Physical and Engineering Sciences*, *376*(2132), 20170406.
684 https://doi.org/10.1098/rsta.2017.0406
685 Stolper, E. (1982). The speciation of water in silicate melts. *Geochimica et Cosmochimica*
686 *Acta*, *46*(12), 2609–2620. https://doi.org/10.1016/0016-7037(82)90381-7
687 Stolper, E., & Holloway, J. R. (1988). Experimental determination of the solubility of carbon
688 dioxide in molten basalt at low pressure. *Earth and Planetary Science Letters*, *87*(4),
689 397–408. https://doi.org/10.1016/0012-821X(88)90004-0
690 Tamic, N., Behrens, H., & Holtz, F. (2001). The solubility of H2O and CO2 in rhyolitic melts
691 in equilibrium with a mixed CO2-H2O fluid phase. *Chemical Geology*, *174*(1–3), 333–
692 347. https://doi.org/10.1016/S0009-2541(00)00324-7
693 Webster, J. D., Goldoff, B., & Shimizu, N. (2011). C–O–H–S fluids and granitic magma: how
694 S partitions and modifies CO2 concentrations of fluid-saturated felsic melt at 200 MPa.

695 *Contributions to Mineralogy and Petrology*, *162*(4), 849–865.
696 https://doi.org/10.1007/s00410-011-0628-1
697 Wyllie, P. J. (1971). Role of water in magma generation and initiation of diapiric uprise in the
698 mantle. *Journal of Geophysical Research (1896-1977)*, *76*(5), 1328–1338.
699 https://doi.org/10.1029/JB076i005p01328
700

TABLES

Table 1. Expected chemical composition (in wt.% unless otherwise indicated) of all experiments based on loaded amounts of starting material.

Sample Name	SiO_2	TiO_2	Al_2O_3	FeO_{tot}	MnO	MgO	CaO	Na_2O	K_2O	P_2O_5	H_2O	CO_2 (ppm)	S (ppm)	Cl (ppm)	F (ppm)	Total
ND 70_ Degassed	50.18	0.85	16.54	8.18	0.17	8.44	13.18	2.21	0.17	0.09	0.00	0	0	0	0	100
ND70-2-01	48.74	0.82	16.06	7.95	0.17	8.28	13.01	2.20	0.17	0.08	2.25	665	672	679	717	100
ND70-3-01	48.15	0.81	15.87	7.85	0.16	8.21	12.95	2.21	0.16	0.08	3.13	989	1001	1011	1067	100
ND70-4-01	47.26	0.80	15.58	7.71	0.16	8.18	13.01	2.26	0.16	0.08	3.99	1970	1993	2013	2125	100
ND70-4-02	47.15	0.80	15.54	7.69	0.16	8.16	12.98	2.25	0.16	0.08	4.22	1965	1988	2008	2120	100
ND70-5-02	47.27	0.71	13.88	6.87	0.14	7.67	13.27	2.33	0.14	0.07	5.01	10349	5072	5468	5497	100
ND70-5-03	48.17	0.81	15.88	7.85	0.16	8.13	12.71	2.14	0.16	0.08	3.82	197	200	202	213	100
ND70-6-02	44.29	0.67	13.01	6.43	0.13	7.71	14.06	2.64	0.13	0.07	6.28	15023	10177	10363	10112	100

Table 2. Experimental conditions.

Experiment #	Pressure (MPa)	Temperature (°C)	Duration (h)
ND 70_ Degassed	0.1	1350	4
ND70-2-01	1000	1325	2
ND70-3-01	1000	1325	2
ND70-4-01	1000	1225	2
ND70-4-02	1000	1325	2
ND70-5-02	1500	1325	2
ND70-5-03	1500	1325	2
ND70-6-02	1500	1325	2

708 **Table 3**. Measured major and volatile composition by electron microprobe (in wt.% unless otherwise indicated) of experimental glasses and other
709 glasses analysed during the same analytical sessions. n denotes the number of analyses from which averages are reported. Errors (two standard
710 deviation) are ±0.43 for SiO_2, ±0.18 for Na_2O, ±0.02 for K_2O, ±0.17 for Al_2O_3, ±0.36 for CaO, ±0.24 for FeO, ±0.11 for MgO, ±0.04 for TiO_2,
711 ±0.05 for MnO, ±0.04 for P_2O_5, ±0.01 for S and ±0.03 for Cl.

	EMPA (AMNH)													
Experiment #	n	SiO_2	TiO_2	Al_2O_3	FeO_{tot}	MnO	MgO	CaO	Na_2O	K_2O	P_2O_5	S (ppm)	Cl (ppm)	Total
ND 70_ Degassed	5	49.68	0.80	16.12	8.27	0.14	8.71	13.01	2.22	0.16	0.09	15	19	99.19
ND70-2-01	10	47.81	0.76	15.58	8.00	0.15	8.51	12.66	2.17	0.17	0.08	621	753	96.02
ND70-3-01	10	47.18	0.77	15.21	8.04	0.15	8.61	12.76	2.09	0.16	0.08	814	1176	95.23
ND70-4-01	10	47.37	0.75	15.13	7.60	0.16	8.23	12.30	2.19	0.16	0.07	1831	2670	94.39
ND70-4-02	10	44.27	0.73	14.54	7.59	0.14	8.23	12.60	2.21	0.16	0.09	1796	2269	90.97
ND70-5-02	10	46.12	0.65	13.21	6.83	0.12	7.89	13.15	2.34	0.15	0.07	5045	7081	91.75
ND70-6-02	12	44.01	0.64	12.62	6.19	0.11	8.22	13.16	2.12	0.18	0.08	8786	12449	89.46
Other glasses analysed														
ND-70 (Natural)	3	49.92	0.81	16.11	8.17	0.15	8.27	12.95	2.10	0.16	0.09	871	199	98.84
VILLA_P2	12	50.60	1.29	15.42	9.15	0.16	5.41	8.55	3.10	0.75	0.28	3529	120	95.08
INSOL_MX1_BA4	1	52.36	1.62	12.87	8.12	0.11	9.55	10.53	2.66	1.41	0.23	18	114	99.48

712

713

714

715 **Table 4**. ERDA, NRA, EA and FTIR measurements (in wt.% for H_2O and in ppm for all other species) of experimental glasses and other glasses
716 analysed during the same analytical sessions. All errors are given as one standard deviation, n denotes the number of analyses from which averages
717 are reported.

	ERDA (CEA-CNRS-Saclay)			NRA (CEA-CNRS-Saclay)			EA (LDEO)			FTIR (LDEO)					EMPA (Caltech)		
Experiment #	n	H_2O	±	n	CO_2	±	n	CO_2	±	n	H_2O	±	CO_2	±	n	CO_2	±
ND 70_ Degassed																	
ND70-2-01	2	2.53	0.24	1	1837	35				6	2.12	0.34	1283	120			
ND70-3-01	2	3.13	0.30	1	2689	54				7	3.43	0.97	2226	403	5	2886	428
ND70-4-01	1	4.25	0.40	1	4228	71				8	3.86	0.89	4095	621			
ND70-4-02	2	3.68	0.35	1	4122	65									5	4210	403
ND70-5-02	2	5.34	0.51	1	12682	105	1	12160	891	6	5.34	3.20	12276	4850	5	11106	795
ND70-5-03	1	3.68	0.35														
ND70-6-02	2	6.26	0.59	1	16847	120	1	14940	1095	3	5.85	0.96	15754	1835	5	13403	164
Other glasses analysed																	
ND-70 (Natural)										3	0.66	0.15	59	23			
Suprasil	2	0.02	0.00														
BF73	2	0.73	0.07	1	2832	56				3	0.82	0.06	3042	84	5	6508	4175
BF76										3	0.75	0.06	2319	68	5	3455	219
BF77										3	0.86	0.08	891	47	5	2390	231
M19															5	5112	424
M20	1	5.82	0.55	1	2417	51									5	2945	1309
M35	1	4.31	0.41	1	1436	40				3	4.1	0.45	1000	75	5	3010	3704
M43										3	2.52	0.25	2857	154	5	3193	520
ALV1846-9										3	1.43	0.12	18	8			
NS-1										3	0.35	0.03	3546	129	5	4616	400
Villa_P2										6	3.92	0.7	835	74			
INSOL_MX1_BA4										3	0.15	0.01	8207	377			

718

719

720 **Table 5**. SIMS measurements (in wt.% for H_2O and in ppm for all other species) of experimental glasses and other glasses analysed during the
721 same analytical sessions. Errors are calculated using two standard error (i.e., 95% confidence interval) on calibration lines for each session, n
722 denotes the number of analyses from which averages are reported. Values in red were determined outside calibration range.
723

	SIMS (CNRS-Nancy, Cs+beam)										
Experiment #	n	H_2O	±	CO_2	±	S	±	Cl	±	F	±
ND 70_ Degassed	2	0.03	0.00	66	6	17	1	4	0	13	1
ND70-2-01	3	2.21	0.06	1141	101	649	42	876	110	572	40
ND70-3-01	2	2.70	0.07	1397	124	862	56	983	124	745	52
ND70-4-01	2	3.79	0.10	2519	224	2207	142	2401	302	1896	133
ND70-5-02	2	4.57	0.12	6566	583	6211	400	6777	852	5538	388
ND70-5-03	2	3.37	0.09	1098	98	175	11	326	41	228	16
ND70-6-02	2	6.37	0.17	6482	576	11214	722	12405	1559	9725	681
Other glasses analysed											
ND-70 (Natural)	1	1.04	0.03	195	17	916	59	194	24	98	7
M34	3	5.59	0.15	458	41	11	1	36	4	79	6
M35	10	4.14	0.11	1100	98	11	1	33	4	75	5
M40	10	3.31	0.09	2118	188	12	1	33	4	73	5
M43	1	2.70	0.07	3071	273	5	0	29	4	68	5
M48	10	0.82	0.02	477	42	3	0	28	4	64	4
KL2	10	0.01	0.00	157	14	6	0	14	2	58	4
KE12	10	0.16	0.00	116	10	264	17	3419	430	4251	298
40428	9	0.88	0.02	256	23	889	57	349	44	413	29
47963	10	1.23	0.03	229	20	646	42	902	113	638	45
N72	5	0.02	0.00	186	17	4	0	28	4	77	5
VG2	10	0.34	0.01	396	35	1450	93	233	29	160	11
	SIMS (WHOI, Cs+beam)										
Experiment #	n	H_2O	±	CO_2	±	S	±	Cl	±	F	±

ND70-2-01	3	2.31	0.10	1204	92	476	57	518	14	550	47
ND70-3-01	2	2.59	0.12	2106	160	582	70	708	20	683	58
ND70-4-01	3	4.16	0.19	3037	231	1553	187	2125	59	1808	155
ND70-4-02	3	3.69	0.17	3026	231	1505	181	1811	50	1665	142
ND70-5-02	3	5.31	0.24	8770	668	4714	567	6357	177	5694	487
ND70-5-03	3	3.85	0.17	1412	108	128	15	300	8	217	19
ND70-6-02	3	7.11	0.32	8216	626	8525	1026	11713	326	10177	870
Other glasses analysed											
ND-70 (Natural)	3	1.02	0.05	120	9	625	75	160	4	86	7
Suprasil	3	0.01	0.00	25	2	0	0	1912	53	3	0
BF73	2	0.87	0.04	2502	191	0	0	36	1	36	3
BF76	2	0.82	0.04	2134	163	0	0	34	1	27	2
BF77	3	0.82	0.04	791	60	0	0	34	1	27	2
M15	3	1.64	0.07	152	12	1	0	21	1	53	5
M19	3	3.06	0.14	2608	199	3	0	21	1	54	5
M20	3	5.76	0.26	1689	129	8	1	25	1	62	5
M34	3	5.52	0.25	332	25	6	1	24	1	60	5
M35	3	4.41	0.20	896	68	5	1	24	1	60	5
M43	3	2.76	0.13	2720	207	2	0	23	1	55	5
M48	3	0.76	0.03	298	23	0	0	19	1	50	4
KE12	3	0.20	0.01	5	0	204	25	3287	92	4220	361
ALV519-4-1	5	0.19	0.01	205	16	614	74	39	1	62	5
80-1-3	3	0.64	0.03	532	41	596	72	47	1	161	14
1846-9	4	1.78	0.08	9	1	236	28	206	6	269	23
NS-1	3	0.42	0.02	4295	327	31	4	24	1	60	5
Villa_P2	3	4.67	0.21	946	72	3638	438	106	3	144	12
INSOL_MX1_BA4	3	0.22	0.01	8314	634	8	1	81	2	271	23
Run101@2.asc	3	1.93	0.09	55	4	285	34	570	16	268	23
Run10@2.asc	3	4.35	0.20	23	2	20	2	401	11	4	0
ALV_1833-1	3	2.28	0.10	15	1	497	60	553	15	254	22

WOK28-3	3	0.52	0.02	292	22	650	78	45	1	95	8
	SIMS (Caltech, Cs+beam)										
Experiment #	n	H_2O	±	CO_2	±	S	±	Cl	±	F	±
ND70-2-01	2	2.49	0.09	1183	117	513	84	859	156	1247	99
ND70-3-01	8	3.18	0.12	1851	184	745	122	1527	277	1828	145
ND70-4-02	3	2.99	0.11	2039	202	1219	199	2061	374	2658	210
ND70-5-02	2	4.94	0.18	8151	808	4687	766	8955	1626	12118	959
ND70-6-02	2	6.95	0.26	7234	718	7687	1257	15406	2798	20358	1611
Other glasses analysed											
ND-70 (Natural)	2	1.09	0.04	135	13	657	107	257	47	193	15
Suprasil	2	0.00	0.00	2	0	0	0	2456	446	0	0
BF73	2	0.79	0.03	2435	242	0	0	53	10	73	6
BF76	2	0.85	0.03	2534	251	0	0	54	10	61	5
BF77	2	0.83	0.03	853	85	0	0	51	9	57	5
M15	2	1.68	0.06	138	14	1	0	32	6	115	9
M19	2	3.41	0.13	2520	250	3	1	35	6	122	10
M20	2	5.36	0.20	1609	160	8	1	39	7	132	10
M34	1	5.40	0.20	265	26	6	1	34	6	124	10
M35	2	4.15	0.15	869	86	5	1	34	6	126	10
M43	1	2.80	0.10	2834	281	2	0	35	6	121	10
M48	1	0.84	0.03	221	22	0	0	31	6	113	9
ALV519-4-1	2	0.16	0.01	189	19	541	88	46	8	111	9
1846-12	2	1.38	0.05	126	12	617	101	347	63	282	22
80-1-3	2	0.55	0.02	365	36	566	93	60	11	317	25
1846-9	2	1.71	0.06	7	1	223	36	275	50	574	45
NS-1	3	0.42	0.02	4931	489	32	5	36	6	135	11
Villa_P2	2	4.52	0.17	909	90	3698	604	151	27	303	24
INSOL_MX1_BA4	2	0.18	0.01	7737	767	6	1	95	17	492	39
Run101@2.asc	2	1.74	0.06	49	5	252	41	781	142	548	43

Run10@2.asc	2	3.78	0.14	14	1	16	3	482	88	2	0

	SIMS (WHOI, O-beam)				
Experiment #	n	H_2O	±	CO_2	±
ND70-2-01	3	2.70	0.11	1315	148
ND70-3-01	5	3.31	0.14	1721	193
ND70-4-01	5	4.21	0.18	3595	404
ND70-4-02	3	3.49	0.15	3219	362
ND70-5-02	3	4.62	0.19	10855	1220
ND70-5-03	3	3.79	0.16	1655	186
ND70-6-02	3	5.96	0.25	11981	1346
Other glasses analysed					
ND-70 (Natural)	3	1.12	0.05	163	18
Suprasil	3	0.01	0.00	30	3
M20	3	5.49	0.23	1851	208
M35	3	4.10	0.17	927	104
ALV519-4-1	3	0.20	0.01	215	24
NS-1	3	0.48	0.02	4254	478
Villa_P2	3	4.26	0.18	1040	117
INSOL_MX1_BA4	3	0.24	0.01	7718	867
	SIMS (Caltech, O-beam)				
Experiment #	n	H_2O	±	CO_2	±
ND70-2-01	2	2.42	0.15	1343	184
ND70-3-01	8	3.05	0.19	1979	271
ND70-4-02	3	3.40	0.21	3309	454
ND70-5-02	2	4.31	0.26	9928	1361
ND70-6-02	2	5.26	0.32	11615	1593
Other glasses analysed					
ND-70 (Natural)					
Suprasil	1	0.00	0.00	0	0

M43	1	2.58	0.16	2806	385
80-1-3	2	0.68	0.04	626	86
NS-1	3	0.45	0.03	4223	579
INSOL_MX1_BA4	2	0.23	0.01	7729	1060

724

725

726

727

728 **Table 6**. Major element and volatile content of the new reference glasses. See text for error on each measurement.

	Majors (normalized)											Volatiles									
Experiment #	SiO_2	TiO_2	Al_2O_3	FeO_{tot}	MnO	MgO	CaO	Na_2O	K_2O	P_2O_5	sum	H_2O	±	CO_2 (ppm)	±	S (ppm)	±	Cl (ppm)	±	F (ppm)	±
ND 70_ Degassed	50.09	0.80	16.25	8.34	0.14	8.78	13.11	2.23	0.16	0.09	100	blank		blank		16	1	11	11	13	na
ND-70 (Natural)	50.56	0.82	16.32	8.27	0.15	8.38	13.12	2.13	0.16	0.09	100	0.99	0.19	134	51	767	148	185	21	92	8
ND70-2-01	49.86	0.79	16.25	8.34	0.16	8.87	13.20	2.26	0.17	0.08	100	2.39	0.22	1560	392	565	83	716	182	561	16
ND70-3-01	49.64	0.81	16.00	8.46	0.15	9.06	13.42	2.20	0.17	0.08	100	3.06	0.34	2600	339	751	123	956	235	714	44
ND70-4-01	50.43	0.80	16.10	8.09	0.17	8.76	13.09	2.33	0.17	0.07	100	4.05	0.21	4161	94	1864	328	2399	272	1852	62
ND70-4-02	48.88	0.80	16.05	8.39	0.16	9.09	13.92	2.43	0.18	0.10	100	3.46	0.33	4166	62	1507	288	2040	324	1665	na
ND70-5-02	50.94	0.72	14.59	7.55	0.13	8.72	14.52	2.58	0.16	0.08	100	5.02	0.36	12373	274	5165	717	6738	363	5616	110
ND70-6-02	50.39	0.73	14.45	7.09	0.13	9.41	15.06	2.43	0.21	0.09	100	6.42	0.51	15847	957	9053	1515	12189	413	9951	319

729

SUPPLEMENTARY to: "ND70-series basaltic glass reference materials for volatile element (H2O, CO2, S, Cl, F) analyses and the C ionization efficiency supressing effect of water in silicate glasses."

Yves Moussallam[1], William Henry Towbin[2], Terry Plank[1], Hélène Bureau[3], Hicham Khodja[4], Yunbin Guan[5], Chi Ma[5], Michaael B. Baker[5], Edward M. Stolper[5], Fabian U. Naab[6], Brian D. Monteleone[7], Glenn G. Gaetani[7], Hyun Joo Lee[1], Shuo Ding[1], Sarah Shi[1], Estelle F. Rose-Koga[8].

[1] Lamont-Doherty Earth Observatory, Columbia University, New York, USA

[2] Gemological Institute of America, 50 W. 47th Street, New York, NY 10036, United States of America

[3] IMPMC, Sorbonne Université, CNRS UMR 7590, MNHN, IRD UR 206, 4 place Jussieu, 75252 Paris Cedex 05, France

[4] LEEL, NIMBE, CEA, CNRS, Université Paris−Saclay, CEA Saclay, 91191 Gif sur Yvette Cedex, France

[5] Division of Geological and Planetary Sciences, California Institute of Technology, Pasadena, California 91125, USA

[6] Department of Nuclear Engineering and Radiological Sciences, University of Michigan, Ann Arbor, Michigan 48109, USA

[7] Department of Geology and Geophysics, Woods Hole Oceanographic Institution, Woods Hole, MA 02543, USA.

[8] ISTO, UMR 7327, CNRS-UO-BRGM, 1A rue de la Férollerie, 45071 Orléans cedex 2, France

Corresponding author: Yves Moussallam; yves.moussallam@ldeo.columbia.edu

SUPPLEMENTARY FIGURES

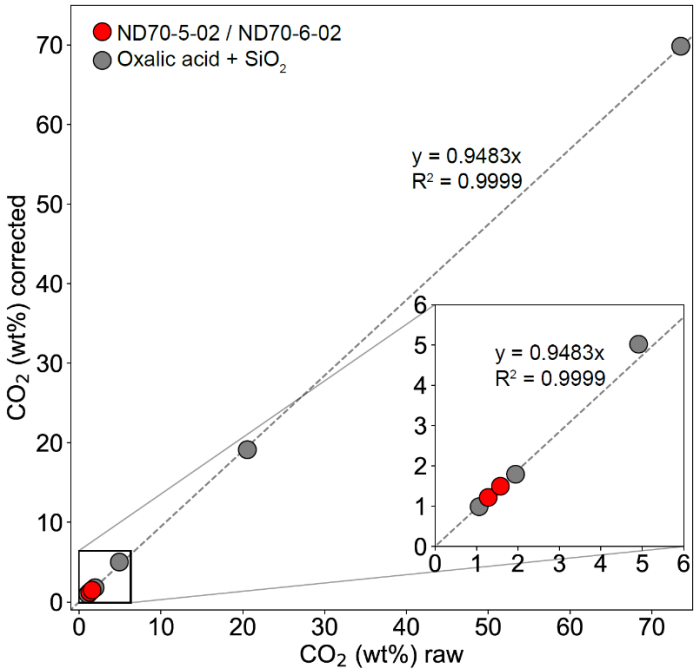

***Figure S1**: Elemental Analyser secondary calibration. CO_2 (wt%) raw indicates the raw EA result calibrated by acetanilide. CO_2 (wt%) corrected is calibrated by a series of oxalic acid and SiO_2 mixtures. Gray circles are oxalic acid and SiO_2 mixtures. Red circles are ND70_5_02 and ND70_6_02. Dashed line is the calibration line based on oxalic acid and SiO_2.*

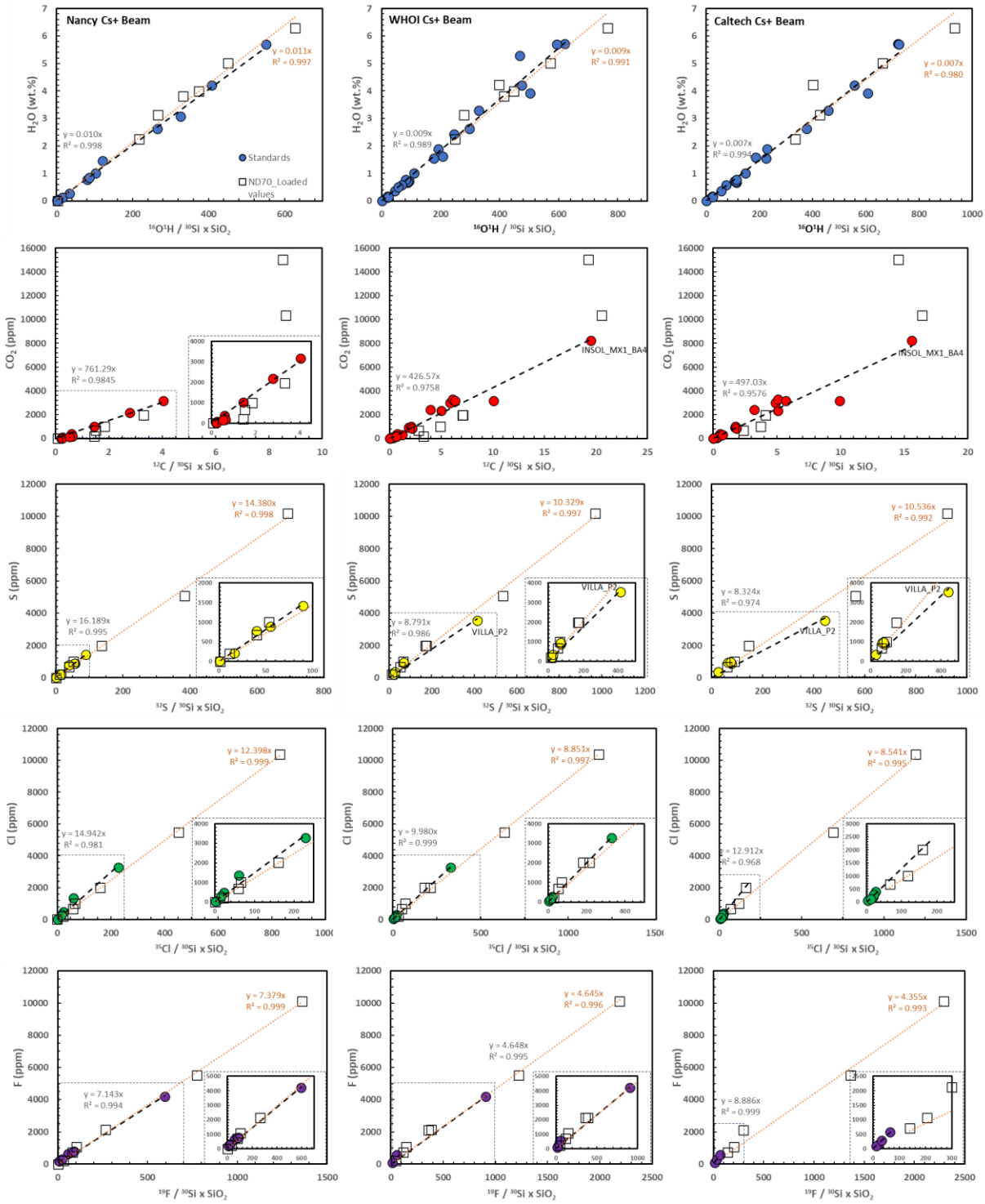

761

762 ***Figure S2***: *Signal retrieved by SIMS using a Cs^+ primary beam at Nancy, WHOI and Caltech*
763 *Ion Probe facilities. Filled circle symbols show glasses used as standards for volatile analyses*
764 *(marked as "Other glasses analysed" in Table 5) in addition to INSOL_MX1_BA and*
765 *VILLA_YM whose volatile content was determined in this study. Square symbols represent the*
766 *new ND70 reference series plotted on the y-axes according to their expected (i.e., loaded)*

767 *values. Data in Tables S3 to S5. Black dashed lines are the calibration lines while red dotted*
768 *lines are linear regressions through the ND series glasses.*

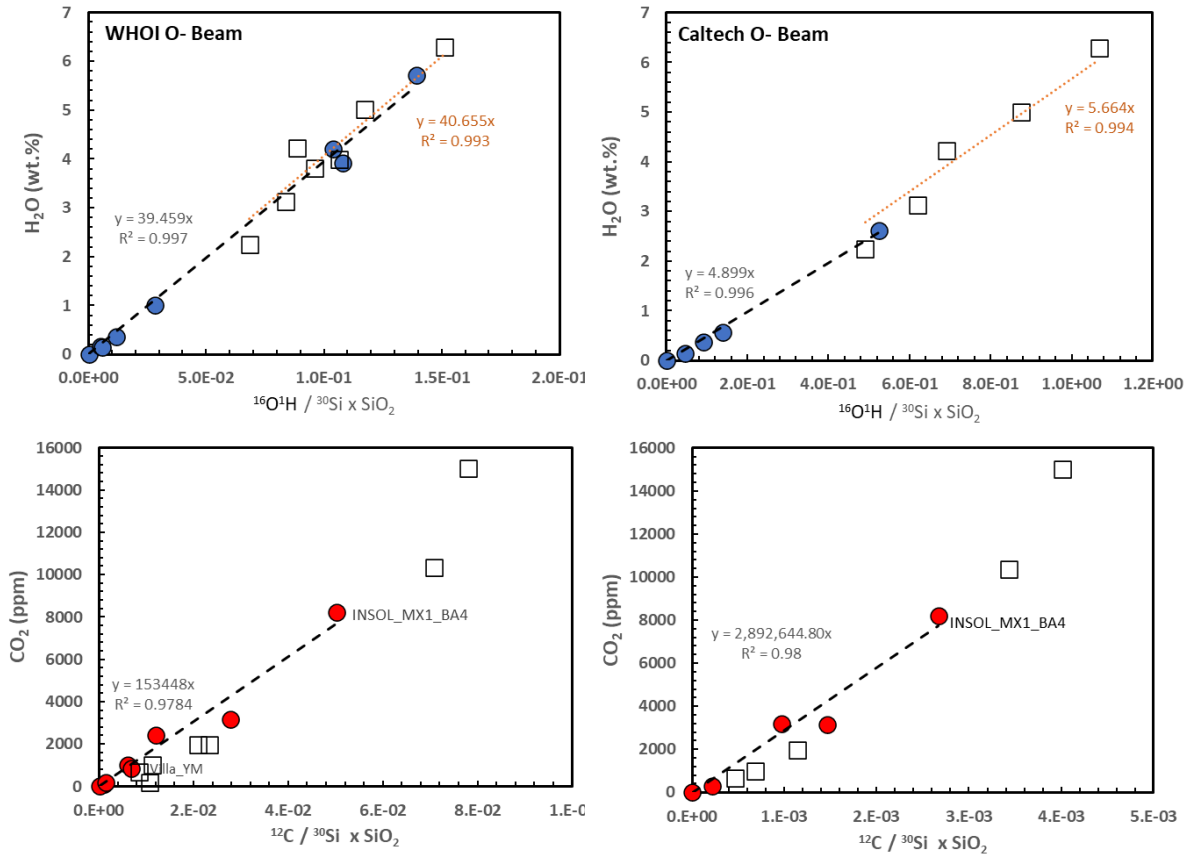

769

770 ***Figure S3****: Signal retrieved by SIMS using a O⁻ primary beam at WHOI and Caltech Ion Probe*
771 *facilities. Filled circle symbols show glasses used as standards for volatile analyses (marked*
772 *as "Other glasses analysed" in Table 5) in addition to INSOL_MX1_BA and VILLA_YM whose*
773 *volatile content was determined in this study. Square symbols represent the new ND70*
774 *reference series plotted on the y-axes according to their expected (i.e., loaded) values. Data in*
775 *Tables S6 and S7. Black dashed lines are the calibration lines while red dotted lines are linear*
776 *regressions through the ND series glasses.*

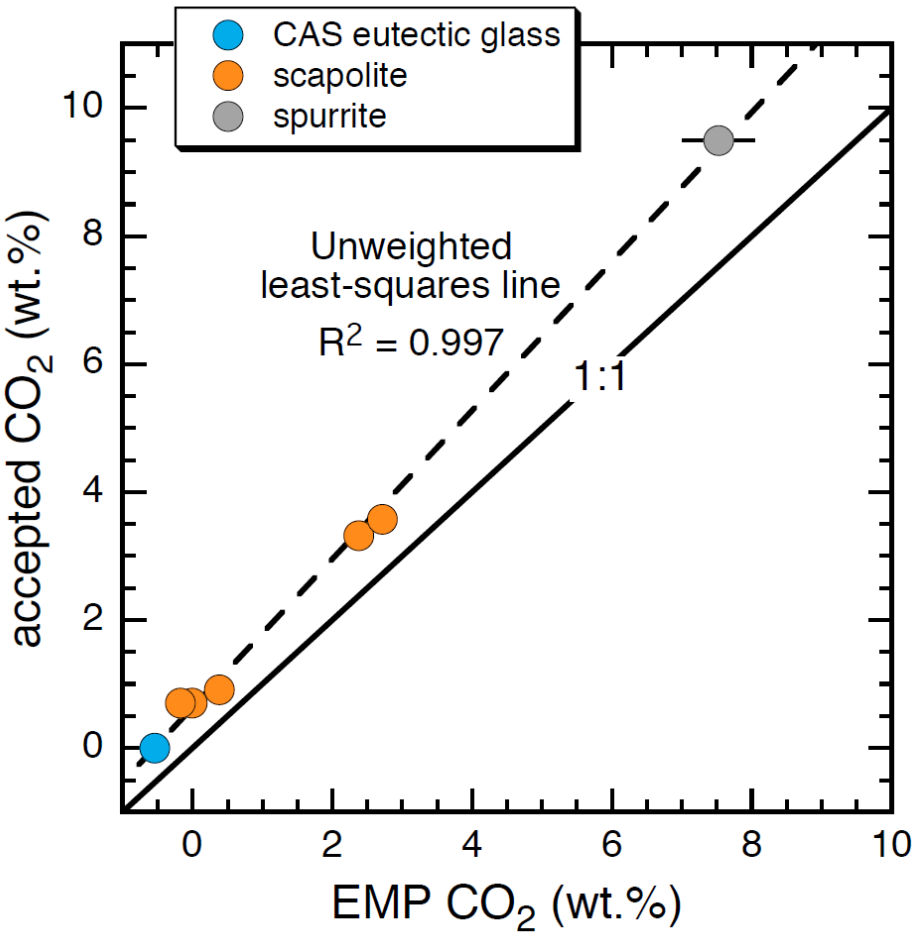

***Figure S4**: Electron microprobe CO_2 contents vs. accepted CO_2 contents (all in wt.%) for the secondary standards. Error bars on the average EMP values are 2σ and where not visible are smaller than the size of the symbols. The CaO-Al_2O_3-SiO_2 eutectic is bounded by the pseudowollastonite, anorthite, and tridymite liquidus fields; the glass was fused at 1-atm in air and is assumed to have a CO_2 content of zero. Scapolite CO_2 contents determined by NRA; the CO_2 content of the spurrite is based on mineral stoichiometry. The dashed line is an unweighted least-squares fit to the seven secondary standards.*

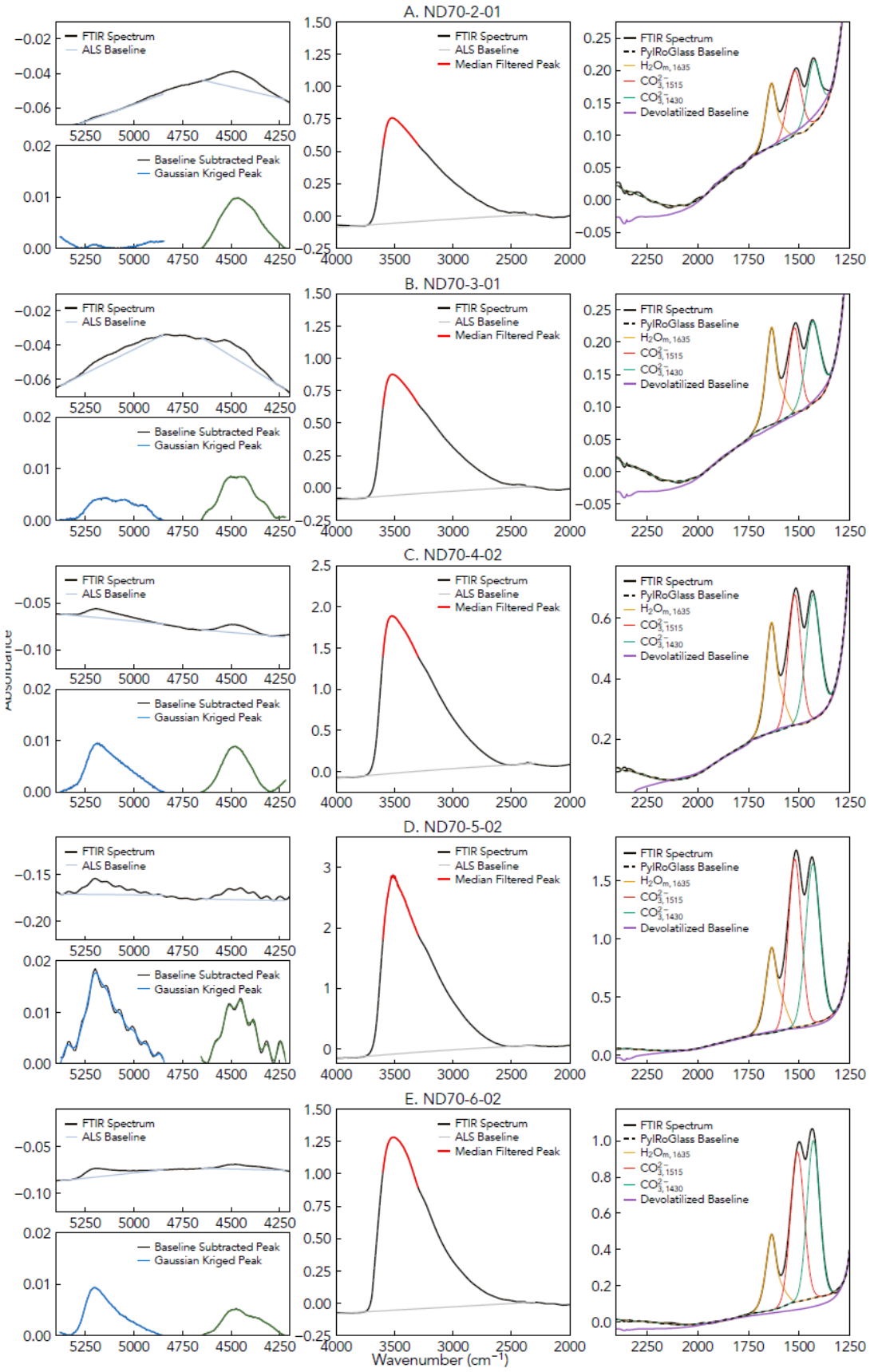

786

787 ***Figure S5****: FTIR spectra of ND70 series glasses and spectra fitting with the PyIRoGlass*
788 *software (Shi et al., in review).*

SUPPLEMENTARY TABLES

Table S1*: Weight of all starting materials added to each experiment. 'ND70-4 Bulk Enriched' is a mixture of all the dry components, mixed for 1 hour, and used as starting material for five of the experiments.*

Experiments and pre-mix	ND70 mix (g)	ND70-4 Bulk Enriched (g)	ND70 + 6wt% SiO2 Mix (g)	Water (g)	Calcite (g)	$CaSO_4$ (g)	NaCl (g)	MgF_2 (g)	Total (g)
ND70-4 Bulk Enriched	0.56770				0.00270	0.00510	0.00200	0.00210	0.57960
ND70-4-01		0.19200		0.00790					0.19990
ND70-4-02		0.19280		0.00840					0.20120
ND70-3-01	0.07310	0.07320		0.00470					0.15100
ND70-2-01	0.13080	0.06550		0.00450					0.20080
ND70-5-03	0.12468	0.01400		0.00550					0.14418
ND70-5-02			0.17790	0.01000	0.00470	0.00430	0.00180	0.00180	0.20050
ND70-6-02			0.16615	0.01250	0.00680	0.00860	0.00340	0.00330	0.20075

796 ***Table S2****: Volatile and SiO_2 contents (normalised to 100%) of other glasses analysed.*

Name	H_2O (wt.%)	CO_2 (ppm)	F (ppm)	S (ppm)	Cl (ppm)	SiO_2 (wt.%)	References
ND-70	1.015	76.5	148	880	184	50.4	Keller et al., 2008; Caulfield et al., 2012; Lloyd et al., 2013
Suprasil	0.0007±0.0002	0.65±0.35	0.19±0.05	0.15±0.03	1000-3000	100.0	(Shimizu et al., 2021)
BF73	0.72	2995				51.2	Brounce et al., 2021 and Almeev (unpublished)
BF76	0.67	2336				51.2	Brounce et al., 2021 and Almeev (unpublished)
BF77	0.70	935				51.2	Brounce et al., 2021 and Almeev (unpublished)
M15	1.54	60				50.5	Shishkina et al., 2010
M19	3.29	3277				50.4	Shishkina et al., 2010
M20	5.72	2421				50.4	Shishkina et al., 2010
M34	5.70	375				50.4	Shishkina et al., 2010
M35	4.20	1019				50.4	Shishkina et al., 2010
M40	3.07	2183				50.3	Shishkina et al., 2010
M43	2.62	3172				50.4	Shishkina et al., 2010
M48	0.77	176				51.0	Shishkina et al., 2010
KL2	0.02	5	177	8	26	50.1	Jochum et al., 2006; Rose-Koga et al., 2020
KE12	0.12		4200	210	3280	70.8	Mosbah et al., 1991 and Mandeville (unpublished); Rose-Koga et al., 2020
40428	0.85		650	890	494	51.0	Kamenetsky et al., 2000
47963	1.45		777	776	1356	48.9	Kamenetsky et al., 2000
N72	0.00	0				50.1	Shishkina et al., 2010
ALV519-4-1	0.17	165	95	950	53	49.1	Bryan & Moore, 1977; Hauri et al., 2002; Kumamoto et al., 2017 and Hauri (unpublished)
1846-12	1.58	90	288	981	400	50.8	Newman et al., 2000; Hauri et al., 2002; Kumamoto et al., 2017
80-1-3	0.57	295				48.9	Newman et al., 2000; Kumamoto et al., 2017 and Hauri (unpublished)
1846-9	1.89	0	574	358	292	49.7	Newman et al., 2000; Kumamoto et al., 2017 and Hauri (unpublished)
NS-1	0.37	3154				50.4	Helo et al., 2011
VILLA_P2	3.92	835		3529	120	53.4	This study

INSOL_MX1_BA4	0.15	8207				52.6	This study
VG2	0.28	153	300	1424	298	50.8	Jarosewich et al., 1980; Rose-Koga et al., 2020
Run101	1.62					57.6	Mandeville et al., 2002
Run10	5.28					57.2	Mandeville et al., 2002

797

798 ***Table S3**: Raw SIMS analyses from IMS 1280 at CNRS-CRPG Nancy using a Cs+ primary beam.*

	SIMS (CNRS-Nancy) Cs+ primary beam																				
Experiment #	n	$^{12}C/^{30}Si$	±	$^{16}O^{1}H/^{30}Si$	±	$^{19}F/^{30}Si$	±	$^{32}S/^{30}Si$	±	$^{35}Cl/^{30}Si$	±	$^{12}C/^{18}O$	±	$^{16}O^{1}H/^{18}O$	±	$^{19}F/^{18}O$	±	$^{32}S/^{18}O$	±	$^{35}Cl/^{18}O$	±
ND 70_ Degassed	2	0.0017	0.0002	0.0578	0.0012	0.0371	0.0022	0.0206	0.0010	0.0048	0.0003	0.0019	0.0001	0.0641	0.0016	0.0403	0.0004	0.0225	0.0001	0.0053	0.0000
ND70-2-01	3	0.0301	0.0024	4.3713	0.1936	1.6094	0.1119	0.8055	0.0434	1.1781	0.0666	0.0265	0.0006	3.9555	0.0437	1.4228	0.0162	0.7207	0.0029	1.0494	0.0045
ND70-3-01	2	0.0370	0.0029	5.3718	0.2615	2.1066	0.1490	1.0753	0.0591	1.3283	0.0789	0.0334	0.0006	4.9536	0.0399	1.9056	0.0232	0.9821	0.0036	1.2108	0.0038
ND70-4-01	2	0.0659	0.0052	7.4514	0.3509	5.2887	0.3632	2.7161	0.1416	3.2016	0.1763	0.0509	0.0010	5.8959	0.0509	4.1039	0.0434	2.1256	0.0139	2.5017	0.0109
ND70-5-02	2	0.1716	0.0156	8.9640	0.5286	15.4225	1.2157	7.6321	0.4503	9.0217	0.5759	0.1291	0.0034	6.9094	0.0465	11.6824	0.1666	5.8729	0.0246	6.8998	0.0253
ND70-5-03	2	0.0287	0.0022	6.6193	0.2875	0.6352	0.0416	0.2154	0.0106	0.4339	0.0231	0.0230	0.0004	5.4222	0.0601	0.5123	0.0051	0.1751	0.0013	0.3521	0.0015
ND70-6-02	2	0.1731	0.0144	12.7743	0.7299	27.6741	2.1188	14.0800	0.7245	16.8742	1.0217	0.1176	0.0026	8.8323	0.0859	18.8701	0.2968	9.7299	0.1092	11.6021	0.0616
Other glasses analyzed																					
ND-70 (Natural)	1	0.0051	0.0004	2.0414	0.0575	0.2716	0.0160	1.1220	0.0501	0.2579	0.0123	0.0047	0.0001	1.9267	0.0418	0.2528	0.0024	1.0512	0.0068	0.2413	0.0014
M34	3	0.0119	0.0008	10.9312	0.3698	0.2182	0.0117	0.0140	0.0007	0.0473	0.0024	0.0075	0.0002	6.9359	0.0813	0.1370	0.0012	0.0088	0.0001	0.0297	0.0003
M35	10	0.0287	0.0023	8.1092	0.3131	0.2083	0.0132	0.0133	0.0009	0.0433	0.0026	0.0191	0.0005	5.5323	0.0789	0.1401	0.0016	0.0089	0.0001	0.0292	0.0002
M40	10	0.0553	0.0038	6.4981	0.2218	0.2035	0.0119	0.0146	0.0008	0.0433	0.0023	0.0390	0.0008	4.6534	0.0716	0.1441	0.0014	0.0103	0.0001	0.0307	0.0002
M43	1	0.0801	0.0052	5.2770	0.1683	0.1883	0.0105	0.0060	0.0004	0.0384	0.0017	0.0591	0.0009	3.9509	0.0685	0.1395	0.0010	0.0044	0.0001	0.0286	0.0002
M48	10	0.0123	0.0012	1.5927	0.0447	0.1759	0.0114	0.0030	0.0003	0.0367	0.0023	0.0104	0.0004	1.3923	0.0358	0.1510	0.0017	0.0025	0.0001	0.0316	0.0002
KL2	10	0.0041	0.0004	0.0219	0.0007	0.1619	0.0110	0.0070	0.0004	0.0182	0.0012	0.0039	0.0002	0.0213	0.0005	0.1548	0.0022	0.0067	0.0001	0.0175	0.0002
KE12	10	0.0021	0.0003	0.2162	0.0098	8.4050	0.6110	0.2303	0.0118	3.2320	0.1966	0.0019	0.0001	0.2081	0.0025	7.9613	0.1329	0.2217	0.0017	3.0826	0.0170
40428	9	0.0066	0.0006	1.6951	0.0724	1.1336	0.0846	1.0777	0.0625	0.4579	0.0286	0.0067	0.0002	1.7806	0.0228	1.1611	0.0170	1.1142	0.0033	0.4723	0.0021
47963	10	0.0061	0.0005	2.4869	0.1206	1.8266	0.1300	0.8160	0.0479	1.2350	0.0758	0.0063	0.0002	2.5894	0.0262	1.8830	0.0251	0.8410	0.0027	1.2689	0.0061
N72	5	0.0049	0.0005	0.0335	0.0008	0.2143	0.0114	0.0047	0.0004	0.0380	0.0018	0.0040	0.0002	0.0281	0.0007	0.1762	0.0016	0.0039	0.0001	0.0314	0.0002
VG2	10	0.0102	0.0008	0.6600	0.0183	0.4403	0.0292	1.7624	0.0888	0.3069	0.0169	0.0098	0.0003	0.6536	0.0163	0.4263	0.0054	1.7223	0.0081	0.2989	0.0009

799

800

801

802 ***Table S4****: Raw SIMS analyses from IMS 7f-GEO at Caltech using a Cs+ primary beam.*

	SIMS (Caltech) Cs+ primary beam																				
Experiment #	n	$^{12}C/^{30}Si$	±	$^{16}O^{1}H/^{30}Si$	±	$^{19}F/^{30}Si$	±	$^{32}S/^{30}Si$	±	$^{35}Cl/^{30}Si$	±	$^{12}C/^{18}O$	±	$^{16}O^{1}H/^{18}O$	±	$^{19}F/^{18}O$	±	$^{32}S/^{18}O$	±	$^{35}Cl/^{18}O$	±
ND70-2-01	2	0.0478	0.0002	6.7317	0.0170	2.8197	0.0226	1.2384	0.0183	1.3360	0.0411	0.0274	0.0002	3.8655	0.0188	1.6202	0.0175	0.7144	0.0123	0.7708	0.0255
ND70-3-01	8	0.0752	0.0054	8.6127	0.3426	4.1524	0.1505	1.8058	0.0625	2.3865	0.0928	0.0391	0.0013	4.5398	0.2608	2.1764	0.0452	0.9468	0.0357	1.2517	0.0445
ND70-4-02	3	0.0843	0.0035	8.2648	0.2507	6.1457	0.2329	3.0092	0.0691	3.2802	0.0749	0.0584	0.0009	5.7656	0.0102	4.2917	0.0403	2.1238	0.0137	2.3185	0.0307
ND70-5-02	2	0.3262	0.0021	13.2015	0.1969	27.1263	0.0998	11.2017	0.0430	13.7957	0.1175	0.1476	0.0007	6.0019	0.1567	12.3280	0.1835	5.1213	0.0792	6.3053	0.1274
ND70-6-02	2	0.2958	0.0164	18.9729	1.2590	46.5657	2.3499	18.7704	0.2025	24.2523	0.3967	0.1269	0.0022	8.1747	0.2270	20.0705	0.2322	8.1458	0.2286	10.5244	0.2328
Other glasses analysed																					
ND-70 (Natural)	2	0.0054	0.0001	2.9097	0.1264	0.4307	0.0127	1.5644	0.0070	0.3944	0.0239	0.0033	0.0000	1.7813	0.0463	0.2637	0.0030	0.9605	0.0215	0.2420	0.0102
Suprasil	2	0.0000	0.0000	0.0013	0.0000	0.0002	0.0000	0.0000	0.0000	1.9023	0.0447	0.0000	0.0000	0.0008	0.0000	0.0001	0.0000	0.0000	0.0000	1.2669	0.0439
BF73	2	0.0957	0.0020	2.0744	0.0498	0.1612	0.0021	0.0001	0.0000	0.0798	0.0004	0.0602	0.0005	1.3135	0.0162	0.1015	0.0000	0.0001	0.0000	0.0503	0.0004
BF76	2	0.0996	0.0062	2.2367	0.1879	0.1336	0.0086	0.0003	0.0001	0.0815	0.0029	0.0570	0.0014	1.2869	0.0571	0.0764	0.0019	0.0002	0.0000	0.0467	0.0003
BF77	2	0.0335	0.0016	2.1690	0.1154	0.1254	0.0049	0.0006	0.0000	0.0773	0.0033	0.0205	0.0005	1.3339	0.0408	0.0766	0.0012	0.0004	0.0000	0.0473	0.0010
M15	2	0.0055	0.0003	4.4695	0.0615	0.2567	0.0040	0.0015	0.0003	0.0486	0.0004	0.0032	0.0001	2.5973	0.0324	0.1492	0.0016	0.0009	0.0001	0.0283	0.0005
M19	2	0.1005	0.0002	9.0987	0.0086	0.2719	0.0064	0.0076	0.0006	0.0532	0.0030	0.0540	0.0007	4.8984	0.0450	0.1465	0.0019	0.0041	0.0003	0.0288	0.0013
M20	2	0.0642	0.0010	14.2935	0.0897	0.2936	0.0007	0.0201	0.0003	0.0594	0.0001	0.0287	0.0003	6.4065	0.0023	0.1316	0.0005	0.0090	0.0002	0.0266	0.0001
M34	1	0.0106	0.0002	14.3829	0.1797	0.2767	0.0040	0.0135	0.0003	0.0530	0.0013	0.0051	0.0001	6.9973	0.0547	0.1347	0.0009	0.0066	0.0001	0.0258	0.0004
M35	2	0.0347	0.0021	11.0667	0.9776	0.2818	0.0101	0.0113	0.0001	0.0527	0.0001	0.0169	0.0007	5.3833	0.3833	0.1373	0.0024	0.0055	0.0002	0.0258	0.0005
M43	1	0.1132	0.0018	7.4751	0.0851	0.2707	0.0047	0.0041	0.0001	0.0541	0.0012	0.0604	0.0003	3.9914	0.0142	0.1445	0.0008	0.0022	0.0000	0.0289	0.0003
M48	1	0.0087	0.0001	2.2129	0.0203	0.2501	0.0034	0.0001	0.0000	0.0465	0.0009	0.0054	0.0001	1.3672	0.0064	0.1545	0.0006	0.0001	0.0000	0.0288	0.0003
ALV519-4-1	2	0.0077	0.0007	0.4490	0.0260	0.2550	0.0104	1.3248	0.0014	0.0734	0.0003	0.0059	0.0003	0.3438	0.0072	0.1951	0.0006	1.0234	0.0385	0.0567	0.0025
1846-12	2	0.0050	0.0001	3.6540	0.0268	0.6252	0.0128	1.4597	0.0264	0.5293	0.0107	0.0034	0.0000	2.4897	0.0160	0.4257	0.0024	1.0009	0.0026	0.3631	0.0017
80-1-3	2	0.0150	0.0011	1.5076	0.0055	0.7287	0.0087	1.3904	0.0159	0.0952	0.0012	0.0104	0.0009	1.0467	0.0104	0.5050	0.0003	0.9694	0.0224	0.0663	0.0016
1846-9	2	0.0003	0.0000	4.6133	0.1971	1.3004	0.0560	0.5399	0.0081	0.4284	0.0065	0.0002	0.0000	2.8100	0.0058	0.7901	0.0019	0.3305	0.0083	0.2625	0.0066
NS-1	3	0.1969	0.0106	1.1232	0.0394	0.3005	0.0064	0.0758	0.0034	0.0548	0.0033	0.1216	0.0048	0.6996	0.0155	0.1861	0.0048	0.0472	0.0025	0.0341	0.0023
VILLA_P2	2	0.0344	0.0024	11.4049	0.3284	0.6406	0.0226	8.3473	0.3511	0.2201	0.0090	0.0165	0.0006	5.6285	0.0236	0.3084	0.0011	4.1159	0.3091	0.1063	0.0010
INSOL_MX1_BA4	2	0.2957	0.0073	0.4497	0.0080	1.0520	0.0288	0.0128	0.0007	0.1404	0.0022	0.2117	0.0021	0.3262	0.0056	0.7595	0.0052	0.0094	0.0008	0.1026	0.0018

803

804 ***Table S5****: Raw SIMS analyses from IMS 1280 at WHOI using a Cs+ primary beam.*

	SIMS (WHOI) Cs+ primary beam										
Experiment #	n	12C/30Si	±	16O1H/30Si	±	19F /30Si	±	32S /30Si	±	35Cl /30Si	±
ND70-2-01	3	0.0567	0.0013	4.9908	0.0825	2.3760	0.0294	1.0878	0.0068	1.0433	0.0213
ND70-3-01	2	0.0997	0.0029	5.6332	0.1643	2.9645	0.1933	1.3357	0.1003	1.4319	0.1657
ND70-4-01	3	0.1419	0.0023	8.9285	0.0868	7.7497	0.0527	3.5208	0.0274	4.2429	0.0406
ND70-4-02	3	0.1458	0.0010	8.1725	0.0150	7.3624	0.0271	3.5184	0.0232	3.7283	0.0346
ND70-5-02	3	0.4089	0.0086	11.3843	0.2507	24.3667	0.2252	10.6667	0.0273	12.6703	0.1309
ND70-5-03	3	0.0658	0.0010	8.2423	0.1151	0.9277	0.0155	0.2896	0.0039	0.5979	0.0132
ND70-6-02	3	0.3915	0.0024	15.5580	0.3396	44.5050	0.4786	19.7107	0.2466	23.8557	0.4052
Other glasses analysed											
ND-70 (Natural)	3	0.0056	0.0001	2.1747	0.0161	0.3684	0.0028	1.4098	0.0059	0.3185	0.0018
Suprasil	3	0.0006	0.0009	0.0078	0.0021	0.0075	0.0002	0.0002	0.0002	1.9159	0.0178
BF73	2	0.1145	0.0093	1.8283	0.0315	0.1505	0.0009	0.0006	0.0007	0.0708	0.0009
BF76	2	0.0977	0.0009	1.7173	0.0153	0.1142	0.0002	0.0004	0.0001	0.0675	0.0003
BF77	3	0.0362	0.0002	1.7300	0.0153	0.1140	0.0009	0.0007	0.0000	0.0662	0.0006
M15	3	0.0071	0.0012	3.5002	0.0535	0.2273	0.0016	0.0016	0.0001	0.0414	0.0006
M19	3	0.1212	0.0029	6.5289	0.0298	0.2316	0.0015	0.0064	0.0003	0.0414	0.0009
M20	3	0.0785	0.0020	12.3073	0.1822	0.2660	0.0026	0.0176	0.0003	0.0499	0.0012
M34	3	0.0155	0.0027	11.7937	0.0590	0.2563	0.0012	0.0125	0.0002	0.0479	0.0005
M35	3	0.0417	0.0013	9.4117	0.0320	0.2542	0.0031	0.0105	0.0003	0.0472	0.0007
M43	3	0.1266	0.0008	5.9117	0.0665	0.2360	0.0010	0.0037	0.0000	0.0450	0.0010
M48	3	0.0137	0.0073	1.6145	0.0207	0.2119	0.0017	0.0003	0.0002	0.0382	0.0007
KE12	3	0.0002	0.0001	0.3022	0.0169	12.8230	0.0459	0.3286	0.0102	4.6523	0.0382
ALV519-4-1	5	0.0098	0.0001	0.4117	0.0044	0.2708	0.0025	1.4244	0.0153	0.0802	0.0015
80-1-3	3	0.0255	0.0098	1.3997	0.0357	0.7085	0.0095	1.3856	0.0028	0.0955	0.0025
NS-1	3	0.1999	0.0077	0.8877	0.0229	0.2543	0.0028	0.0694	0.0009	0.0482	0.0006
VILLA_P2	3	0.0416	0.0012	9.4519	0.0758	0.5811	0.0041	7.7760	0.6566	0.1994	0.0036
INSOL_MX1_BA4	3	0.3703	0.0102	0.4441	0.0574	1.1063	0.0570	0.0176	0.0045	0.1534	0.0106

Run101@2.asc	3	0.0022	0.0001	3.6113	0.0404	1.0030	0.0281	0.5635	0.0188	0.9911	0.0370
Run10@2.asc	3	0.0009	0.0001	8.1861	0.1171	0.0166	0.0005	0.0400	0.0016	0.7018	0.0189
ALV_1846-9	4	0.0004	0.0000	3.8590	0.0445	1.1673	0.0093	0.5410	0.0053	0.4149	0.0064
ALV_1833-1	3	0.0007	0.0000	4.5644	0.1128	1.0142	0.0067	1.0499	0.0241	1.0283	0.0224
WOK28-3	3	0.0137	0.0002	1.1325	0.0089	0.4112	0.0025	1.4849	0.0155	0.0901	0.0012

805

806

807 ***Table S6****: Raw SIMS analyses from IMS 7f-GEO at Caltech using a O- primary beam.*

	SIMS (Caltech) O- primary beam				
Experiment #	n	$^{12}C/^{30}Si$	±	$^{16}O^{1}H/^{30}Si$	±
ND70-2-01	2	9.32E-06	1.25E-07	9.86E-03	1.11E-04
ND70-3-01	2	1.38E-05	1.43E-06	1.25E-02	1.11E-04
ND70-4-02	2	2.35E-05	1.90E-06	1.42E-02	2.97E-04
ND70-5-02	2	6.83E-05	5.76E-07	1.74E-02	1.59E-04
ND70-6-02	2	8.16E-05	2.48E-07	2.17E-02	6.33E-04
Other glasses analysed					
Suprasil	1	0.00E+00	2.07E-06	0.00E+00	1.53E-08
M43	2	1.93E-05	2.99E-07	1.04E-02	9.22E-06
80-1-3	1	4.42E-06	1.05E-05	2.84E-03	1.69E-07
NS-1	2	2.90E-05	4.28E-07	1.82E-03	1.83E-04
INSOL_MX1_BA4	1	5.08E-05	1.12E-05	8.93E-04	2.52E-07

808

809

***Table S7**: Raw SIMS analyses from IMS 1280 at WHOI using a O- primary beam.*

	SIMS (WHOI) O- primary beam										
Experiment #	n	12C/30Si	±	16O1H/30Si	±	19F /30Si	±	32S /30Si	±	35Cl /30Si	±
ND70-2-01	3	1.72E-04	4.14E-06	1.37E-03	1.09E-05	2.42E-02	2.08E-04	1.56E-03	1.73E-05	5.49E-04	5.16E-06
ND70-3-01	5	2.26E-04	1.20E-05	1.70E-03	3.89E-05	3.44E-02	2.91E-04	1.86E-03	1.92E-05	9.77E-04	2.01E-05
ND70-4-01	5	4.67E-04	1.13E-05	2.12E-03	4.06E-05	6.83E-02	6.44E-04	2.90E-03	5.77E-05	1.93E-03	4.47E-05
ND70-4-02	3	4.31E-04	5.71E-06	1.82E-03	2.31E-05	6.22E-02	5.18E-04	2.82E-03	9.30E-06	1.61E-03	2.41E-05
ND70-5-02	3	1.41E-03	2.04E-05	2.33E-03	7.00E-05	1.90E-01	5.93E-03	6.40E-03	1.38E-04	5.11E-03	2.39E-04
ND70-5-03	3	2.15E-04	1.88E-06	1.91E-03	1.44E-05	8.23E-03	1.69E-04	9.08E-04	8.60E-06	2.74E-04	3.87E-06
ND70-6-02	3	1.59E-03	1.99E-05	3.07E-03	1.44E-04	3.65E-01	1.20E-02	1.10E-02	5.96E-04	1.04E-02	6.60E-04
Other glasses analysed											
ND-70 (Natural)	3	2.10E-05	2.16E-06	5.64E-04	1.76E-05	3.63E-03	6.44E-05	1.73E-03	3.48E-05	1.73E-04	4.53E-06
Suprasil	3	1.97E-06	6.47E-07	2.43E-06	1.05E-06	1.64E-06	5.55E-07	4.60E-07	1.71E-07	3.01E-04	1.99E-05
M20	3	2.39E-04	2.30E-06	2.76E-03	8.94E-05	2.04E-03	6.06E-05	6.50E-04	1.64E-05	4.84E-05	2.47E-06
M35	3	1.20E-04	3.70E-06	2.06E-03	1.95E-05	1.93E-03	5.58E-06	5.10E-04	1.47E-05	3.69E-05	1.27E-06
ALV519-4-1	3	2.85E-05	1.02E-06	1.03E-04	4.84E-06	2.65E-03	7.42E-05	1.83E-03	3.79E-05	5.41E-05	5.31E-06
NS-1	3	5.50E-04	7.34E-06	2.40E-04	3.43E-06	2.56E-03	5.11E-05	8.66E-04	2.83E-05	4.02E-05	3.77E-06
VILLA_P2	3	1.27E-04	3.12E-06	2.03E-03	8.22E-05	3.71E-03	1.31E-04	3.17E-03	1.32E-04	7.54E-05	4.91E-06
INSOL_MX1_BA4	3	9.55E-04	9.31E-05	1.15E-04	1.80E-05	1.22E-02	1.87E-03	7.98E-04	4.14E-05	1.10E-04	1.28E-05

REFERENCES

Brounce, M., Reagan, M. K., Kelley, K. A., Cottrell, E., Shimizu, K., & Almeev, R. (2021). Covariation of Slab Tracers, Volatiles, and Oxidation During Subduction Initiation. *Geochemistry, Geophysics, Geosystems*, *22*(6), e2021GC009823. https://doi.org/10.1029/2021GC009823

Bryan, W. B., & Moore, J. G. (1977). Compositional variations of young basalts in the Mid-Atlantic Ridge rift valley near lat 36°49′N. *GSA Bulletin*, *88*(4), 556–570. https://doi.org/10.1130/0016-7606(1977)88<556:CVOYBI>2.0.CO;2

Caulfield, J., Turner, S., Arculus, R., Dale, C., Jenner, F., Pearce, J., et al. (2012). Mantle flow, volatiles, slab-surface temperatures and melting dynamics in the north Tonga arc–Lau back-arc basin. *Journal of Geophysical Research: Solid Earth*, *117*(B11). https://doi.org/10.1029/2012JB009526

Hauri, E., Wang, J., Dixon, J. E., King, P. L., Mandeville, C., & Newman, S. (2002). SIMS analysis of volatiles in silicate glasses: 1. Calibration, matrix effects and comparisons with FTIR. *Chemical Geology*, *183*(1–4), 99–114. https://doi.org/10.1016/S0009-2541(01)00375-8

Helo, C., Longpré, M.-A., Shimizu, N., Clague, D. A., & Stix, J. (2011). Explosive eruptions at mid-ocean ridges driven by CO2-rich magmas. *Nature Geoscience*, *4*(4), 260–263. https://doi.org/10.1038/ngeo1104

Jarosewich, E., Nelen, J. a., & Norberg, J. A. (1980). Reference Samples for Electron Microprobe Analysis*. *Geostandards Newsletter*, *4*(1), 43–47. https://doi.org/10.1111/j.1751-908X.1980.tb00273.x

Jochum, K. P., Stoll, B., Herwig, K., Willbold, M., Hofmann, A. W., Amini, M., et al. (2006). MPI-DING reference glasses for in situ microanalysis: New reference values for element concentrations and isotope ratios. *Geochemistry, Geophysics, Geosystems*, *7*(2). https://doi.org/10.1029/2005GC001060

Kamenetsky, V. S., Everard, J. L., Crawford, A. J., Varne, R., Eggins, S. M., & Lanyon, R. (2000). Enriched End-member of Primitive MORB Melts: Petrology and Geochemistry of Glasses from Macquarie Island (SW Pacific). *Journal of Petrology*, *41*(3), 411–430. https://doi.org/10.1093/petrology/41.3.411

Keller, N. S., Arculus, R. J., Hermann, J., & Richards, S. (2008). Submarine back-arc lava with arc signature: Fonualei Spreading Center, northeast Lau Basin, Tonga. *Journal of Geophysical Research: Solid Earth*, *113*(B8). https://doi.org/10.1029/2007JB005451

Kumamoto, K. M., Warren, J. M., & Hauri, E. H. (2017). New SIMS reference materials for measuring water in upper mantle minerals. *American Mineralogist*, *102*(3), 537–547. https://doi.org/10.2138/am-2017-5863CCBYNCND

Lloyd, A. S., Plank, T., Ruprecht, P., Hauri, E. H., & Rose, W. (2013). Volatile loss from melt inclusions in pyroclasts of differing sizes. *Contributions to Mineralogy and Petrology*, *165*(1), 129–153. https://doi.org/10.1007/s00410-012-0800-2

Mandeville, C. W., Webster, J. D., Rutherford, M. J., Taylor, B. E., Timbal, A., & Faure, K. (2002). Determination of molar absorptivities for infrared absorption bands of H2O in andesitic glasses. *American Mineralogist*, *87*(7), 813–821. https://doi.org/10.2138/am-2002-0702

Mosbah, M., Metrich, N., & Massiot, P. (1991). PIGME fluorine determination using a nuclear microprobe with application to glass inclusions. *Nuclear Instruments and Methods in Physics Research Section B: Beam Interactions with Materials and Atoms*, *58*(2), 227–231. https://doi.org/10.1016/0168-583X(91)95592-2

Newman, S., Stolper, E., & Stern, R. (2000). H2O and CO2 in magmas from the Mariana arc and back arc systems. *Geochemistry, Geophysics, Geosystems*, *1*(5). https://doi.org/10.1029/1999GC000027

Rose-Koga, E. F., Koga, K. T., Devidal, J.-L., Shimizu, N., Voyer, M. L., Dalou, C., & Döbeli, M. (2020). In-situ measurements of magmatic volatile elements, F, S, and Cl, by electron microprobe, secondary ion mass spectrometry, and heavy ion elastic recoil detection analysis. *American Mineralogist*, *105*(5), 616–626. https://doi.org/10.2138/am-2020-7221

Shimizu, K., Alexander, C. M. O., Hauri, E. H., Sarafian, A. R., Nittler, L. R., Wang, J., et al. (2021). Highly volatile element (H, C, F, Cl, S) abundances and H isotopic compositions in chondrules from carbonaceous and ordinary chondrites. *Geochimica et Cosmochimica Acta*, *301*, 230–258. https://doi.org/10.1016/j.gca.2021.03.005

Shishkina, T. A., Botcharnikov, R. E., Holtz, F., Almeev, R. R., & Portnyagin, M. V. (2010). Solubility of H2O- and CO2-bearing fluids in tholeiitic basalts at pressures up to 500 MPa. *Chemical Geology*, *277*(1–2), 115–125. https://doi.org/10.1016/j.chemgeo.2010.07.014